

Table 1: Comparison of Tabular Outlier Detection Benchmarks. Besides its scale with 2,446 datasets combined, *MACRODATA*’s three benchmarks – *OddBench*, *OvRBench*, *SynBench*– compare favorably w.r.t. key desiderata: #Datasets, #Samples and #Dim.s: range of number of points and features within datasets; Real/Syn. outliers: whether the outliers are from the real world or synthesized; Seman./Stat. outliers: whether the outliers are semantic anomalies (fraud, fault, etc.) or statistical deviations; Curation filters: whether datasets are extensively vetted and filtered based on beyond-basic criteria; Train/Test splits: whether dataset provides standard splits; Public/Private parts: whether benchmarks both publicly share as well as privately retain the test labels of datasets, the latter part used for maintaining a leaderboard; Semantic tags: whether datasets contain semantic metadata and/or tags; Extensive HP conf.: whether extensive hyperparameter configurations are employed for evaluation.

Benchmark	Year	#Data sets	#Samples range	#Dim.s range	Real/Syn. outliers	Seman./Stat. outliers	Curation filters	Train/Test splits	Pub./Priv. parts	Semantic tags	Extensive HP conf.
Emmott <i>et al.</i> [19]	2015	20	[1000,6000]	[1,200]	Real	Statistical	✓	✗	✗	✗	✓
ODDS [42, 43]	2016	31	[148,7063]	[6,274]	Real	Mixed	✗	✗	✗	✗	✗
DAMI [9]	2016	23	[80,60632]	[3,1555]	Real	Mixed	✗	✗	✗	✗	✓
Steinbuss&Böhm [54]	2021	19	[80,60632]	[5,38]	Synthetic	Statistical	✗	✗	✗	✗	✗
ADBenchmarks [38]	2021	21	[405,619326]	[6,10000]	Real	Mixed	✓	✗	✗	✗	✗
ADBench [26]	2022	57	[80,619326]	[3,1555]	Real	Mixed	✗	✗	✗	✗	✗
OddBench [ours]	2026	790	[1000,1012180]	[3,1024]	Real	Semantic	✓	✓	Both	✓	✓
OvRBench [ours]	2026	856	[1000,2215023]	[2,10935]	Real	Statistical	✓	✓	Both	✓	✓
SynBench [ours]	2026	800	[1000,6000]	[2,100]	Synthetic	Statistical	✓	✓	Pub.	✓	✓

more thorough and statistically robust evaluations. It also supports research directions previously limited by small-scale data, including meta-learning [63, 64] and foundation models for OD [22, 50].

Beyond scale and diversity, *MACRODATA* incorporates several unique features that enhance its rigor and utility for the research community (Table 1). First, we provide standardized train/test splits for each dataset, ensuring consistent evaluation across experiments. Second, we introduce public/private benchmark partitions, and withhold the private split test labels to host an online OD leaderboard, enabling ongoing and fair competition. Third, we annotate datasets with semantic metadata, improving interpretability and providing deeper insights into the nature of the outliers. These features make *MACRODATA* a powerful tool for benchmarking OD methods and a valuable resource for future research.

Finally, we conduct extensive experiments on *MACRODATA* across classical, deep, and foundation models for OD, systematically exploring a wide range of hyperparameter configurations. This large-scale evaluation provides a comprehensive assessment, highlighting statistically significant performance differences and providing insights for both researchers and practitioners.

The following summarizes our main contributions.

- **“Demystfying” ADBench:** Despite its small scale, which limits its representativeness and statistical power for evaluation, ADBench has become the de facto standard for OD. We critically analyze its limitations, revealing that it primarily captures global outliers resembling Gaussian noise.
- **New Large-scale OD Benchmarks:** We introduce *MACRODATA*, a comprehensive, open-source repository featuring 2,446 datasets from three distinct testbeds: *OddBench*, with real-world datasets containing semantic anomalies; *OvRBench*, with real-world datasets containing statistical outliers; and *SynBench*, containing synthetically generated datasets from diverse priors and outlier archetypes. Owing to its scale, diversity, train/test splits, public/private partitions, and rich metadata, *MACRODATA* meets key desiderata, providing a standardized and robust foundation for OD evaluation.

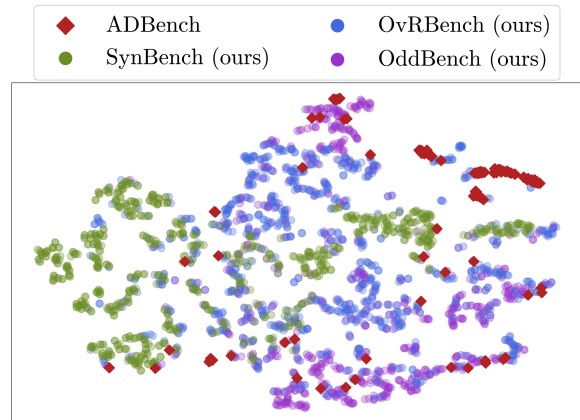


Figure 1: t-SNE embedding of datasets (based on dataset-level metafeatures [57]) across three *MACRODATA* benchmarks (ours) and from ADBench [26] show that *MACRODATA* offers significant boost in both scale and diversity. (best in color)

- **Evaluation and Practical Guidelines:** We perform extensive evaluations across a wide range of OD methods and hyperparameter configurations, revealing statistically significant performance differences and offering actionable insights for future OD research and practice.
- **Frontiers of OD and Future Opportunities:** *MACRODATA* establishes a rich playground for exploring the future frontiers of OD, including meta-learning and foundation models for OD.

Availability: We open-source (1)–(5), and host an online OD leaderboard at <https://huggingface.co/MacROData-CMU>: (1) **Public datasets** (690+756+800) from *OddBench*, *OvRBench*, *SynBench*, plus performance comparisons of prominent OD methods, (2) **Private datasets** (100+100 from *OddBench* and *OvRBench*) (w/out Test labels), plus Leaderboard metrics, (3) **Code** for dataset curation with detailed filtering criteria, (4) **Code** for dataset construction (given a table, without target; convert to OD task), and (5) **Individual performance results** of all methods on all 2,446 datasets.

2 Related Work and ADBench

2.1 A Brief History on OD

Outlier detection (OD) finds numerous real world applications across domains (finance, medicine, security, to name a few). Therefore, there exists a vast body of detection algorithms, from classical [1, 29] to deep architectures [11, 38]. The plethora of detectors raises the question of which one to use on a new task [56]. Selecting an effective OD algorithm (**and** its hyperparameter values), however, is a challenging task. First, there is often no labeled data for model selection. Second, the track record of progress in the field is not reliable due to limited benchmarks and lack of governing over hyperparameter (HP) configuration, where manual dataset selection and manual HP tuning plague the results, raising concerns for fair evaluation [14, 60].

Various work in the OD literature pointed to the HP sensitivity of both classical methods [2, 25, 35] and deep learning based methods with even more HPs [14], offering workarounds, such as reporting performance averaged across multiple HPs [25] or employing unsupervised model selection heuristics [15, 35, 63]. Several unsupervised hyperparameter optimization (HPO) methods rely on meta-learning on historical data repositories with labels [15, 63, 64], which are also needed for reliable evaluation. More recent foundation models for OD pretrain on labeled datasets, another form of meta-learning [50]. These underscore the need for large-scale, new OD benchmarks [3], not only to keep a reliable record of progress, but also to foster effective HPO and future foundation models.

2.2 Existing OD Benchmarks

Table 1 shows a list of existing OD benchmarks. First, they are only a handful. Most strikingly, they are minuscule; containing only a few tens of datasets.¹ Beyond size, they lack crucial properties that are standard for modern-era benchmarks. We defer a detailed discussion of these properties to Section 3, and briefly mention that unlike proposed MACRODATA, they do not exhibit standard Train/Test splits, extensive curation, semantic tags and metadata, and public/private variants with redacted test labels in the latter for fair, blinded testing. In addition, characteristics and types of outliers in these benchmarks are limited compared to the diversity covered by the three benchmarks in MACRODATA.

Curiously, these benchmarks do not compare in popularity: ADBench [26], specifically, stands out as the **de facto** benchmark that is frequently used for evaluation in the literature. That is possibly because it is the most recent (2022) and the relatively largest (57). Moreover, it combines some of the other earlier benchmarks; borrowing datasets from ODDS (26) [43], DAMI (19) [9], Emmott *et al.* (11) [19], DevNet (6) [39], while also including embeddings of (6) image and (5) text datasets as additional tabular datasets.² Appx. A.1 provides summary statistics of ADBench datasets.

Due to its disproportionate popularity and prominence in the literature, Section 2.3 provides a critical lens into ADBench.

2.3 Demystifying ADBench

In 2024, Livernoche *et al.* [34] introduced the *state-of-the-art* OD algorithm on ADBench called DTE (for Diffusion Time Estimation),

inspired by the latest developments in denoising diffusion. At the time, DTE was shown to outperform a record-breaking number (23) of baselines, from traditional shallow algorithms to deep learning-based methods, including the original DDPM [28]. Yet, curiously, the basic KNN algorithm by Ramaswamy *et al.* [41] is the **second top** performer as reported in Livernoche *et al.* [34].

Most recently, in 2025 Shen *et al.* [50] introduced FoMo-0D, the first foundation model for zero(0)-shot OD, which rivaled DTE [34] (across hyperparameters) and performed statistically no different from KNN [41] (2nd top performer), while being pretrained solely on **synthetic** datasets and requiring **no** additional model training or (the notorious) hyperparameter tuning on a new OD task.

These recent developments and curious observations raise key questions: *What drives the strong performance of these new approaches on ADBench? What makes FoMo-0D achieve as competitive results on ADBench, considering it was pretrained purely on synthetic datasets? How could the basic KNN remain competitive against these modern techniques (that use diffusion and extensive pretraining)? What could these observations reveal about ADBench?*

Appx. A.2 provides our deep-dive on the innerworkings of DTE and FoMo-0D to address these questions, and sheds light on ADBench. We brief our key findings and implications as follows.

2.3.1 Key Findings. The analysis of DTE’s [34] analytical form and its approximation in Appx. A.2.1 establishes intriguing *connections between denoising diffusion time, Gaussian noise variance and nearest neighbors*. Specifically, DTE aims to estimate the posterior distribution over diffusion time of a stochastic process that creates noisy samples over time following a diffusion process. Then, DTE considers diffusion time as a surrogate for the distance from the data manifold, for which they derive an analytical formula under Gaussian noise. Effectively, DTE identifies data points as outliers if their probability is high(er) under a Gaussian distribution with a large(r) variance. In other words, the **assumed outliers mimic Gaussian noise, and resemble global outliers—with diffusion noise variance increasing in the full d -dimensional feature space**, unlike *sub-space* outliers.³

DTE proceeds to approximate the analytical form that yields a function of the distance from a data point to its nearest neighbor (NN) in the dataset. In practice, DTE uses not only the smallest but the squared average distance to KNNs for better approximation, especially for larger time steps. Therefore, their non-parametric approach coined as DTE-NP **produces a ranking (of data points by outlieriness) identical to that by average squared KNN distance, a classical OD approach**. Notably, the KNN algorithm by Ramaswamy *et al.* [41] is slightly different as it uses the largest, i.e. k th NN distance as the outlier score instead of the average.

On the other hand, FoMo-0D [50] is pretrained on datasets synthesized from a Gaussian mixture model (GMM) based data prior. Outliers are sampled from the same GMM used to synthesize the inliers, but with *inflated variances*. Then, FoMo-0D **models outliers as generated by Gaussian noise** similar to DTE that treats outliers as generated by a diffusion process under Gaussian noise.

2.3.2 Take-aways. The peering beneath DTE and FoMo-0D, and understanding their makeup and inner-working have allowed us

¹We list the number of “mother” datasets although some works derive different variants.

²ADBench is criticized for its embeddings of other modalities as tabular data [44].

³See Eq. (3) in Appx. where co-variance matrix is a scaled Identity matrix in $\mathbb{R}^{d \times d}$.

to reveal two key findings. **First**, DTE internally models outliers as generated by Gaussian noise, governed by a diffusion process. This is similar to FoMo-OD, which is pretrained on datasets with outliers simulated from Gaussian noise. **Second**, DTE estimates the distribution over diffusion time (i.e. Gaussian noise variance) approximately using average KNN distances. Together, these findings unify our understanding of why three seemingly different algorithms — DTE-NP [34], KNN [41], FoMo-OD [50] — are similarly competitive, and achieve state-of-the-art performance on ADBench.

2.3.3 Remarks on ADBench. These connections allow us to draw key conclusions about ADBench. First is the revelation that ADBench likely exhibits datasets with outliers that align well with *Gaussian noise*. In addition, these are most likely *global* outliers—points that stand out across many input features—as DTE models noise diffusion in *all* dimensions and KNN measures distances across *all* features indiscriminately.

These insights expose key limitations of ADBench, beyond its scale and other desiderata highlighted in Table 1, suggesting that stress-testing OD algorithms likely requires going beyond global outliers that merely resemble Gaussian noise.

We also critique ADBench with regard to its dataset composition. First, its representativeness is severely hampered by its small number of (57) datasets, hindering reliable ablation studies across varying dataset characteristics; for example, dimensionality, domain, etc. Among its small body of datasets, it includes near-duplicates (e.g., Cardio and Cardiography, or Satellite and Satimage-2 or BreastW and Mammography), which may inadvertently overweigh specific data distributions. In contrast, standard datasets like Arrhythmia are omitted despite their prevalence in the literature. Overall, its dataset selection criteria appear somewhat arbitrary. Curiously, it also contains *non-tabular* data embeddings, which can be criticized [44] as not representing traditional tabular datasets with often raw or hand-crafted features. Outside of embeddings, ADBench is dominated by low-dimensional data; nearly 50% of datasets have fewer than 20 features—biasing evaluation toward methods less affected by the curse of dimensionality.

In addition, the utility of several constituent datasets is hampered by difficulty levels: “trivial” sets like BreastW, Thyroid, Fraud allow most algorithms to achieve >90% ROC AUC, introducing evaluation noise due to performance saturation, while “very hard” sets like Yeast, Vertebral, Speech, IMDb often result in near-random performance (<60% ROC AUC), presenting an unrealistic, overly pessimistic evaluation scenario.

Other concerns include data integrity and reliability; for example, the Thyroid dataset exhibits only five features compared to the standard six found in the UCI repository, and the Wine dataset’s reliance on a mere 10 anomalies makes it statistically unreliable.

Collectively, these observations necessitate a cautious interpretation of results derived from ADBench. The benchmark’s lack of structural diversity and over-representation of narrow outlier characteristics limit its ability to reflect the complexity of real-world anomaly scenarios. Our work aims to fill these gaps by introducing an extensive evaluation suite called MACRODATA that prioritizes scale, diversity, and rigorous curation. Furthermore, we adhere to established evaluation protocols; including standardized train/test splits and the use of both public and private datasets, where the latter enables a blinded, impartial evaluation of OD performance.

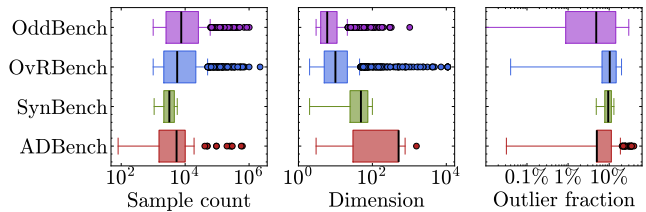


Figure 2: Summary statistics of MACRODATA vs. ADBench.

3 Proposed MACRODATA Benchmarks

Our MACRODATA consists of three separate benchmarks: (1) **OddBench** with 790 *real world* datasets associated with various abnormalities, thus containing *semantic anomalies*, carefully curated from TabLib [17]; (2) **OvRBench** with 856 *real world* datasets curated from TabLib [17] and classification libraries (TabZilla [36], TabRepo [46], TabArena [21], etc.), containing *statistical outliers*; and (3) **SynBench** with 800 *synthetic* datasets generated from five different data priors with *diverse known outlier types*.

MACRODATA provides (i) **scale**; with over two thousand datasets in total⁴ that is two orders of magnitude larger than existing OD benchmarks with only several tens of datasets, and (ii) **diversity**⁵; two real world benchmarks span multiple domains with various semantic tags⁶ and one synthesized benchmark contains datasets with diverse inlier distributions and different known outlier types. Each dataset comes with a **standard Train/Test split**⁷; with inlier-only training data. This enables **both one-class (inductive) and unsupervised (transductive) detection** (with Train/Test combined in the latter). Furthermore, we provide both a **Public&Private benchmark**⁸ of the real-world MACRODATA benchmarks, where private datasets’ test labels are redacted on our end. These private test labels are used to maintain an **online leaderboard** of detectors, enabling a fair and consistent record of progress tracking.⁹

MACRODATA improves upon ADBench in representativeness (Fig. 1, Fig. 2) and introduces key innovations for the first time (Table 1), establishing a comprehensive benchmark that is designed to effectively assess and actively foster progress in the field of OD¹⁰.

3.1 OddBench

3.1.1 Filtering Criteria. The proposed OddBench is based on TabLib [17], which contains 627 million real-world tabular datasets with abundant metadata, extracted from numerous file formats, including CSV, HTML, SQLite, PDF, Excel, and others, sourced from GitHub and Common Crawl. We use half of TabLib to build OddBench, while the other half is used to build OvRBench. Specifically,

⁴Respecting possible resource constraints for benchmarking, we provide 50 representative datasets each, for OddBench, OvRBench and SynBench; see Sec. 3.1.5.

⁵We show both a high semantic diversity; see Fig. 4 and Fig. 6; and a high diversity in dataset characteristics; see Appx. B.1.6, Fig. 11.

⁶We augment each real world dataset with semantic tags, which the practitioners can leverage to scope their evaluation; see Sec. 3.1.3.

⁷We designate random 50% of inliers to Train, and rest 50% inliers plus all outliers to Test. Each dataset includes only one Train/Test split; however, the large number of single-split datasets offsets the effects of particularly un/lucky splits.

⁸We selected 100 random datasets as private from the real-world benchmarks OddBench and OvRBench, and publicly share the rest, 690 and 756 datasets respectively.

⁹As MACRODATA is sourced from public repos, we take preventive steps against reverse-engineering private dataset identities, and thereby their test labels; see Sec. 3.1.4.

¹⁰Supervised algorithms significantly outperform unsupervised algorithms on our benchmarks, signaling large possible improvements; see Appx. B.1.6, Fig. 13.

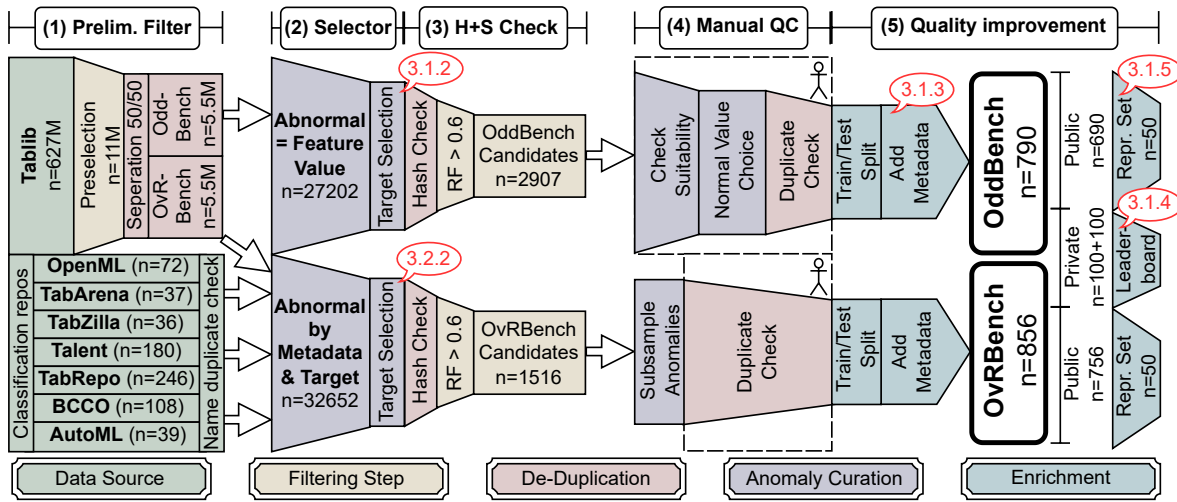


Figure 3: Overview of curation steps used to build OddBench and OvRBench.

OddBench contains a subset of TabLib where positive samples are associated with **semantic anomalies** in the real world. We take the following steps to build OddBench, as outlined in Figure 3.

(1) *Preliminary Filter*: Tablib contains raw Web-sourced tables. First, we remove all clearly unusable datasets; for each raw table, we drop the columns with ratio of null or infinity values above 25%, and any rows that contain null or infinity values. We also drop all monotonous features that might indicate indices. Next, we drop all datasets that contain fewer than 1000 samples or 3 numerical features, and no categorical feature that can be used to assign labels.

(2) *Target-based Filter*: The preliminary selection criteria filter down Tablib by more than an order of magnitude (623M to 11M datasets). From the remaining, we take half for the semantic OddBench while the rest is used for OvRBench. Next, we search for datasets where exactly one categorical feature value is associated with anomaly detection (e.g., “fraud”, “failure”, “defect”; see the full list in Appx. B.1.1). We use samples with this feature value as anomalies and drop other categorical features (Sec. 3.1.2).

(3) *Hash and Separability Check*: We calculate a custom hash code (Appx. B.1.2) for each dataset to remove duplicate datasets and also consider only such datasets where inlier samples can be separated from our anomalies. To that end, we demand that a supervised Random Forest classifier [7] reaches at least 60% ROC-AUC.

(4) *Manual Quality Control*: All remaining 2907 candidate datasets are inspected manually. First, we check if the datasets are truly related to anomaly detection (1300/2907) and select the best-matching inlier categories for each dataset. We also manually remove all duplicate datasets that our earlier hash function missed (790/1300).

(5) *Quality Improvements*: We add Train/Test splits using 50% of inliers as the training and 50% in test set with anomalies, add further metadata (Sec. 3.1.3), retain part of our data as Private for an OD leaderboard (Sec. 3.1.4), and create a representative set of 50 datasets with similar performance distribution (Sec. 3.1.5).

3.1.2 Target Selection. OddBench comprises only those datasets with a categorical feature that explicitly identifies anomalous samples. Appx. B.1.1 details a list of keywords used to select anomalous feature values (e.g., “attack”, “failure”, “error”). Each candidate



(a) OddBench reflects semantic anomalies.(b) OddBench spans real-world domains.

Figure 4: Word clouds of metadata keywords across OddBench datasets showing (a) the semantic anomalies and (b) a broad spectrum of domains covered. Full version is shown in (a), while overly frequent keywords including “anomal”, “status”, “outlier”, “classification”, “data”, “performance”, “failure”, “quality”, “location”, and “error” are dropped in (b).

dataset undergoes manual verification to confirm semantic relevance to the anomaly detection domain and to select the most suitable subset of inlier feature values if multiple are present.

3.1.3 Metadata. To facilitate further research on anomaly detection, each dataset incorporates extensive metadata, comprising of feature names and original source links. We leverage a Large Language Model (LLM) (Appx. B.1.3) to derive descriptive, human-readable titles and relevant keywords. Figure 4 illustrates that OddBench spans various types of semantic anomalies (a), from a variety of real-world domains (b). Furthermore, domain- and dataset-specific tags enable targeted investigations into specialized scenarios, such as high-dimensional or low-sample anomaly detection (Appx. B.1.6, Fig. 12).

3.1.4 Anonymization Efforts. We designate 100 private datasets for a leaderboard to maintain benchmark integrity. Our anonymization pipeline strips all metadata, leaving only raw training and test samples. We further obfuscate each dataset by randomly shuffling both feature and sample order. These, combined with our manual dataset curation, ensure that reverse-engineering the source datasets is prohibitively time-consuming, therefore securing private test labels against de-anonymization.

3.1.5 Representative Set. To curb the computation cost incurred by evaluating a possibly slow detector on hundreds of public datasets,

with multimodality, nonlinearity, non-Gaussian marginals, and heteroscedasticity—properties common in real-world tabular data [40, 48]. They also allow efficient sampling via a single topological pass through an MLP, with cost linear in the number of edges. We instantiate an SCM as a directed acyclic graph $G = (V, E)$, where each node corresponds to a variable and structural equations take the form $X_j = f_j(X_{Pa(X_j; G)}, \epsilon_j)$. We materialize G using an MLP with randomly dropped edges, sample weights, inputs, and exogenous noise from standard Normal distributions, and define each f_j as a weighted sum followed by a random activation. Propagating noise through the graph and reading out a selected subset of nodes $X \subset V$ and target Y yields inlier samples.

We generate two outlier types: measurement and structural outliers. *Measurement outliers* are created by inflating the variance of the exogenous noise at a randomly selected variable, allowing the perturbation to propagate downstream while preserving the causal structure. *Structural outliers* instead modify the causal graph by breaking or reversing edges, thereby altering the underlying data-generating mechanisms. While measurement outliers typically exhibit extreme values, structural outliers are characterized by violations of expected causal dependencies and may not be extreme in magnitude. Outlier severity is controlled via the noise inflation scale and the fraction of intervened edges.

3.3.3 Copulas. We use copula models as a synthetic prior to independently control feature marginals and dependence, motivated by evidence that real-world marginals often exhibit skewed or power-law behavior [12]. By Sklar’s theorem [52], any continuous multivariate distribution decomposes into marginal CDFs and a copula, enabling separate specification of marginals and dependencies. This flexibility allows us to model diverse tabular distributions with non-Gaussian marginals, nonlinear or asymmetric dependence, and tail dependence, beyond covariance-based models [31, 37].

We draw each feature’s marginal independently from a pool of parametric distributions (Gaussian, Beta, Exponential, Student’s t , Power-law, and Log-logistic) and choose either a Gaussian or bivariate vine copula for the dependence structure. Inliers are generated by sampling $\mathbf{u} \sim C$ on $[0, 1]^d$ and transforming each coordinate via $x_j = F_j^{-1}(u_j)$, yielding $\mathbf{x} = (x_1, \dots, x_d)$. We vary marginals, parameters, and copula families to obtain a wide range of datasets. Leveraging the copula decomposition, we construct two outlier types. *Probabilistic outliers* are created by pushing a subset of copula coordinates toward the boundaries (near 0 or 1), producing multivariate extremes that preserve approximate dependence after inverse marginal mapping. *Dependence outliers* disrupt the joint structure by inverting ($u_j \leftarrow 1 - u_j$) or permuting selected coordinates, violating dependencies without necessarily inducing extreme values. Outlier severity is controlled by the fraction of perturbed dimensions and the magnitude of the copula-space perturbations.

4 Evaluation

We design experiments to investigate the following empirical questions, based on which we provide practical guidelines.

- **Q1) Performance:** How do prominent OD methods, from classical to deep to foundation models, compare on MACRODATA?
- **Q2) Running time:** How does running time trade off against performance for different methods?

- **Q3) Hyperparameter sensitivity:** How sensitive are different methods to their HP configuration choices?

We conduct an extensive evaluation on all **2,446** MACRODATA datasets using **14** popular OD methods. The methods are chosen from top-performing approaches identified in prior studies and evaluated across a range of hyperparameter (HP) configurations. We govern experiment design and HP configurations systematically to ensure fair evaluation and to set a standard for the future.

4.1 Experiment Setup

Benchmarked Methods. For competitive evaluation, we take the union of the top-2 OD methods reported in established survey and benchmarking studies [9, 16, 19, 20, 25, 26, 34, 54], covering both **classical** and **deep** models. We also include recent **foundation** models, namely FoMo-OD [50] and OUTFORMER [13] which are specialized in zero-shot tabular OD, and include TabPFN-OD; an adaptation of TabPFN [30] for supervised prediction to OD, by designating each feature as a prediction target and averaging errors across features as the outlier score. See Appx. C.1 and Table 9.

HP Configurations. Most classical and deep models are sensitive to their HP choices as discussed in Sec. 2.1. For fair evaluation, we consider different HP configurations and report average performance and standard deviation to capture performance variability. For shallow models, we consider the full HP grid. For deep models, due to time and memory constraints, we randomly sample five HP settings from the predefined search space. Appx. Table 10 gives detailed HP configurations for classical and deep methods. In contrast, foundation models require no model fitting, thereby no HP-tuning. **Metrics.** We extensively evaluate the baselines on MACRODATA w.r.t. detection performance, runtime, and HP sensitivity. For detection, we report results using both AUROC and AUPRC. Instead of aggregating raw performances across hundreds of datasets with varying difficulty, we report five metrics that better capture relative performance across datasets: Average Rank, ELO [18], Win Rate, rescaled AUROC or AUPRC (rAUC), and Champion Delta (C_Δ) [61]. In addition, we conduct pairwise statistical comparisons between methods and report p -values based on permutation tests. Appx. C.2 gives implementation details. For total running time, we report inference time (only) for foundation models, and model fitting plus inference time for classical and deep models. For HP sensitivity of a baseline, we measure the inter-quartile range of 25%-75% across HP configurations and report its distribution across datasets.

4.2 Results & Guidelines

4.2.1 Main Results. Q1) Performance: Table 2 provides relative AUPRC performance comparison of all baselines across all 2,446 MACRODATA datasets combined. Figure 7 supplements these metrics with paired statistical tests between all 14 baselines. (See Appx. D.1 for results on individual benchmarks, and Appx. D.2 for all corresponding results w.r.t. AUROC.)

Together, Table 2 and Figure 7 show that tabular foundation models (FMs) significantly outperform all classical and deep OD methods, except EGMM [24]. Ensemble-based EGMM is competitive with TABPFN-OD but much slower as shown next, and is significantly outperformed by OUTFORMER. Deep OD models underperform relative to many classical methods, largely due to their hyperparameter (HP) sensitivity, as detailed below.

Table 2: Overall AUPRC performance comparison of OD methods on all 2,446 datasets. Comparisons on individual benchmarks, OddBench, OvRBench, and SynBench, are respectively in Appx. D.1 Tables 14,15 and 16. green, blue, red depict classical, deep, foundation model categories. Best result within category is bolded, with overall best underlined.

	Model	Avg. Rank (↓)	ELO (↑)	Winrate (↑)	rAUC (↑)	C_{Δ} (↓)
Classical	OCSVM	8.15±3.2	370	0.44	0.724±0.21	0.52
	KNN	6.68±3.0	1036	0.55	0.766±0.23	0.45
	LOF	6.20±3.5	1265	0.58	0.773±0.23	0.44
	CBLOF	8.42±3.4	893	0.42	0.676±0.28	0.49
	iForest	9.56±3.9	633	0.34	0.628±0.29	0.55
	EGMM	4.88±3.6	1535	0.68	0.833±0.23	0.34
	DTE-NP	6.12±2.9	1026	0.59	0.783±0.22	0.44
Deep	GOAD	11.17±3.1	674	0.21	0.557±0.28	0.57
	ICL	7.89±3.3	1180	0.44	0.721±0.23	0.50
	DTE-C	6.78±3.5	1090	0.52	0.781±0.23	0.45
	NPT-AD	11.44±3.7	55	0.19	0.517±0.29	0.58
FM	TabPFN-OD	5.22±4.0	1604	0.66	0.822±0.24	0.26
	FoMo-0D	6.20±4.0	1283	0.59	0.800±0.23	0.39
	OutFormer	4.84±3.8	1355	0.69	0.854±0.22	0.29

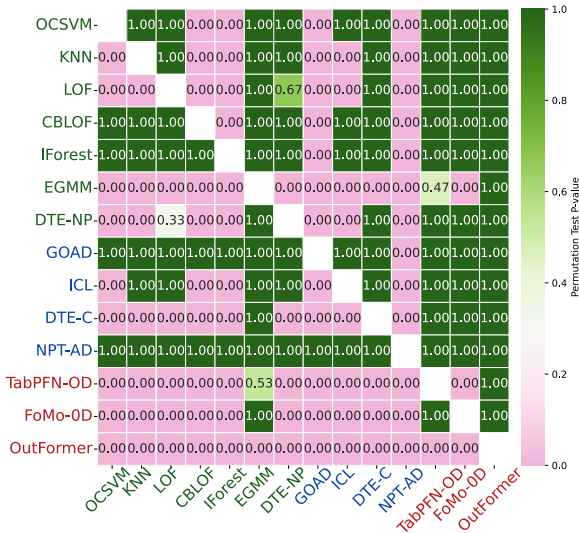


Figure 7: Paired permutation tests on AUPRC across all datasets show the competitiveness of foundation models, with OUTFORMER significantly outperforming all baselines.

Q2) Running time: Figure 8 (left) presents the total running time distribution over all datasets for all methods. In general, classical methods are faster than deep ones, with the exception of EGMM. Feed-forward-only FMs incur the least cost, except TabPFN-OD which iterates over features for prediction. Ensemble-based EGMM that stands out performance-wise is relatively slow, underscoring the typical trade-off in Figure 8 (right). Remarkably, FMs like FoMo-0D and OUTFORMER take the lead in *both* performance and running time—offering the best of both worlds.

Q3) Hyperparameter (HP) sensitivity: Figure 9 shows that performance varies substantially with HP choices across datasets, especially for deep models with many HPs, compared to classical methods with only a few. Ensemble approaches such as iForest

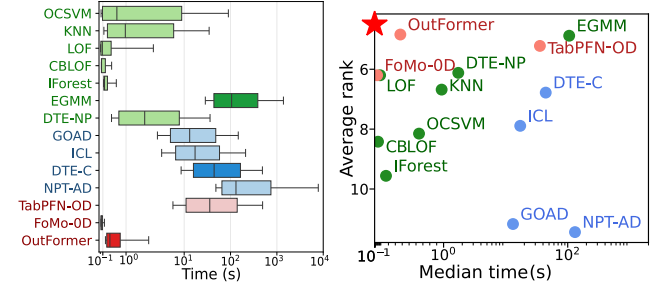


Figure 8: (left) Running time comparison of OD methods across all datasets. (right) Time-vs-Performance trade-off; FM-based FoMo-0D and OUTFORMER occupy the Pareto front.

[32] and EGMM [24] exhibit greater HP robustness, while FMs are especially notable for eliminating the need for tuning altogether.

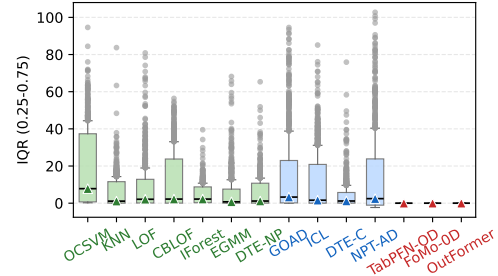


Figure 9: Performance variation across HP configurations (as measured by inter-quartile 25%-75% AUPRC; the higher, the more HP-sensitive) across all datasets (boxplot) per baseline.

4.2.2 Practical Guidelines. Our extensive evaluations firmly position FMs as the dominant approach to OD, excelling in *both* performance and runtime—a rare occurrence. Classical methods typically outperform deep models and offer greater robustness. Among those, EGMM, DTE-NP, and LOF define the performance-runtime Pareto front in Figure 8 (right), where LOF is lightweight and well suited for CPU-only, low-resource settings. FM-based FoMo-0D and OUTFORMER, however, dominate these and occupy the true Pareto front, with model sizes of roughly 5M and 45M parameters; far smaller than the billion-scale language models, and well within the limits of mainstream GPUs. Ultimately, FMs stand at the forefront for practical OD owing to their strong performance, low-latency inference, and truly plug-and-play nature.

5 Conclusion

We introduce MACRODATA, a large-scale benchmark suite for tabular outlier detection (OD), consisting of 2,446 datasets from diverse real-world domains and synthetic inlier/outlier priors, with standardized train/test splits and rich semantic metadata. Besides public datasets, we reserve private subsets and their test labels, supporting an online OD leaderboard. We present extensive experiments across all benchmarks, analyzing performance, runtime, and hyperparameter sensitivity of a select set of OD methods. With its scale and diversity, MACRODATA provides a robust testbed for evaluating OD with enhanced statistical power. Beyond evaluation, our benchmarks, along with data curation and generation strategies, open new research avenues in meta-learning and foundation models for OD, which emerge as the leading-edge frontier.

References

- [1] Charu C. Aggarwal. 2013. *Outlier Analysis*. Springer.
- [2] Charu C. Aggarwal and Saket Sathe. 2015. Theoretical foundations and algorithms for outlier ensembles. *Acm sigkdd explorations newsletter* 17, 1 (2015), 24–47.
- [3] Leman Akoglu. 2021. Anomaly mining: Past, present and future. In *Proceedings of the 30th ACM International Conference on Information & Knowledge Management*. 1–2.
- [4] Lion Bergman and Yedid Hoshen. 2020. Classification-Based Anomaly Detection for General Data. In *International Conference on Learning Representations*.
- [5] Bernd Bischl, Giuseppe Casalicchio, Matthias Feurer, Pieter Gijsbers, Frank Hutter, Michel Lang, Rafael G Mantovani, Jan N van Rijn, and Joaquin Vanschoren. 2017. Openml benchmarking suites. *arXiv preprint arXiv:1708.03731* (2017).
- [6] Stephan Bongers, Patrick Forré, Jonas Peters, and Joris M Mooij. 2021. Foundations of structural causal models with cycles and latent variables. *The Annals of Statistics* 49, 5 (2021), 2885–2915.
- [7] Leo Breiman. 2001. Random Forests. *Mach. Learn.* 45, 1 (Oct. 2001), 5–32. doi:10.1023/A:1010933404324
- [8] Markus M. Breunig, Hans-Peter Kriegel, Raymond T. Ng, and Jörg Sander. 2000. LOF: identifying density-based local outliers. In *Proceedings of the 2000 ACM SIGMOD International Conference on Management of Data (Dallas, Texas, USA) (SIGMOD '00)*. Association for Computing Machinery, New York, NY, USA, 93–104. doi:10.1145/342009.335388
- [9] Guilherme O Campos, Arthur Zimek, Jörg Sander, Ricardo JGB Campello, Barbora Mícenková, Erich Schubert, Ira Assent, and Michael E Houle. 2016. On the evaluation of unsupervised outlier detection: measures, datasets, and an empirical study. *Data mining and knowledge discovery* 30 (2016), 891–927.
- [10] Miguel A. Carreira-Perpinan. 2002. Mode-finding for mixtures of Gaussian distributions. *IEEE Transactions on Pattern Analysis and Machine Intelligence* 22, 11 (2002), 1318–1323.
- [11] Raghavendra Chalapathy and Sanjay Chawla. 2019. Deep learning for anomaly detection: A survey. *arXiv preprint arXiv:1901.03407* (2019).
- [12] Aaron Clauset, Cosma Rohilla Shalizi, and Mark EJ Newman. 2009. Power-law distributions in empirical data. *SIAM review* 51, 4 (2009), 661–703.
- [13] Xueying Ding, Haomin Wen, Simon Klüttermann, and Leman Akoglu. 2026. From Zero to Hero: Advancing Zero-Shot Foundation Models for Tabular Outlier Detection. *arXiv preprint arXiv:2602.03018* (2026).
- [14] Xueying Ding, Lingxiao Zhao, and Leman Akoglu. 2022. Hyperparameter sensitivity in deep outlier detection: Analysis and a scalable hyper-ensemble solution. *Advances in Neural Information Processing Systems* 35 (2022), 9603–9616.
- [15] Xueying Ding, Yue Zhao, and Leman Akoglu. 2024. Fast Unsupervised Deep Outlier Model Selection with Hypernetworks. *ACM SIGKDD* (2024).
- [16] Rémi Domingues, Maurizio Filippone, Pietro Michiardi, and Jihane Zouaoui. 2018. A comparative evaluation of outlier detection algorithms: Experiments and analyses. *Pattern recognition* 74 (2018), 406–421.
- [17] Gus Eggert, Kevin Huo, Mike Biven, and Justin Waugh. 2023. Tablib: A dataset of 627m tables with context. *arXiv preprint arXiv:2310.07875* (2023).
- [18] Arpad E. Elo. 1967. The Proposed USCF Rating System, Its Development, Theory, and Applications. *Chess Life* 22 (1967), 242–247.
- [19] Andrew Emmott, Shubhomoy Das, Thomas Dietterich, Alan Fern, and Weng-Keen Wong. 2015. A meta-analysis of the anomaly detection problem. *arXiv preprint arXiv:1503.01158* (2015).
- [20] Andrew F Emmott, Shubhomoy Das, Thomas Dietterich, Alan Fern, and Weng-Keen Wong. 2013. Systematic construction of anomaly detection benchmarks from real data. In *Proceedings of the ACM SIGKDD workshop on outlier detection and description*. 16–21.
- [21] Nick Erickson, Lennart Purucker, Andrej Tschalzev, David Holzmüller, Prateek Mutalik Desai, David Salinas, and Frank Hutter. 2025. Tabarena: A living benchmark for machine learning on tabular data. *arXiv preprint arXiv:2506.16791* (2025).
- [22] Anurag Garg, Muhammad Ali, Noah Hollmann, Lennart Purucker, Samuel Müller, and Frank Hutter. 2025. Real-TabPFN: Improving Tabular Foundation Models via Continued Pre-training With Real-World Data. *arXiv:2507.03971* [cs.LG] <https://arxiv.org/abs/2507.03971>
- [23] Pieter Gijsbers, Erin LeDell, Janek Thomas, Sébastien Poirier, Bernd Bischl, and Joaquin Vanschoren. 2019. An open source AutoML benchmark. *arXiv preprint arXiv:1907.00909* (2019).
- [24] Michael Glodek, Martin Schels, and Friedhelm Schwenker. 2013. Ensemble Gaussian mixture models for probability density estimation. *Comput. Stat.* 28, 1 (Feb. 2013), 127–138. doi:10.1007/s00180-012-0374-5
- [25] Markus Goldstein and Seichi Uchida. 2016. A comparative evaluation of unsupervised anomaly detection algorithms for multivariate data. *PLoS one* 11, 4 (2016).
- [26] Songqiao Han, Xiyang Hu, Hailiang Huang, Minqi Jiang, and Yue Zhao. 2022. Ad-bench: Anomaly detection benchmark. *Advances in Neural Information Processing Systems* 35 (2022).
- [27] Zengyou He, Xiaofei Xu, and Shengchun Deng. 2003. Discovering Cluster-Based Local Outliers. *Pattern Recogn. Lett.* 24, 9–10 (jun 2003), 1641–1650.
- [28] Jonathan Ho, Ajay Jain, and Pieter Abbeel. 2020. Denoising diffusion probabilistic models. *Advances in Neural Information Processing Systems* 33 (2020), 6840–6851.
- [29] Victoria Hodge and Jim Austin. 2004. A survey of outlier detection methodologies. *Artificial intelligence review* 22, 2 (2004), 85–126.
- [30] Noah Hollmann, Samuel Müller, Katharina Eggenberger, and Frank Hutter. 2023. TabPFN: A Transformer That Solves Small Tabular Classification Problems in a Second. In *The Eleventh International Conference on Learning Representations*.
- [31] Regis Houssou, Mihai-Cezar Augustin, Efstratios Rappos, Vivien Bonvin, and Stephan Robert-Nicoud. 2022. Generation and simulation of synthetic datasets with copulas. *arXiv preprint arXiv:2203.17250* (2022).
- [32] Fei Tony Liu, Kai Ming Ting, and Zhi-Hua Zhou. 2008. Isolation Forest. In *2008 Eighth IEEE International Conference on Data Mining*. 413–422.
- [33] Si-Yang Liu, Hao-Run Cai, Qi-Le Zhou, and Han-Jia Ye. 2024. TALENT: A tabular analytics and learning toolbox. *arXiv preprint arXiv:2407.04057* (2024).
- [34] Victor Livernoche, Vineet Jain, Yashar Hezaveh, and Siamak Ravanbakhsh. 2024. On Diffusion Modeling for Anomaly Detection. In *ICLR*.
- [35] Martin Q Ma, Yue Zhao, Xiaorong Zhang, and Leman Akoglu. 2023. The need for unsupervised outlier model selection: A review and evaluation of internal evaluation strategies. *ACM SIGKDD Explorations Newsletter* 25, 1 (2023), 19–35.
- [36] Duncan McElfresh, Sujay Khandagale, Jonathan Valverde, Vishak Prasad C, Ganesh Ramakrishnan, Micah Goldblum, and Colin White. 2023. When do neural nets outperform boosted trees on tabular data? *Advances in Neural Information Processing Systems* 36 (2023), 76336–76369.
- [37] Roger B Nelsen. 2006. *An introduction to copulas*. Springer.
- [38] Guansong Pang, Chunhua Shen, Longbing Cao, and Anton Van Den Hengel. 2021. Deep learning for anomaly detection: A review. *ACM computing surveys (CSUR)* 54, 2 (2021), 1–38. <https://github.com/mala-lab/ADBenchmarks-anomaly-detection-datasets>
- [39] Guansong Pang, Chunhua Shen, and Anton van den Hengel. 2019. Deep Anomaly Detection with Deviation Networks. In *Proceedings of the 25th ACM SIGKDD International Conference on Knowledge Discovery & Data Mining*. Association for Computing Machinery, New York, NY, USA, 353–362. doi:10.1145/3292500.3330871
- [40] Jonas Peters, Dominik Janzing, and Bernhard Schölkopf. 2017. *Elements of causal inference: foundations and learning algorithms*. The MIT press.
- [41] Sridhar Ramaswamy, Rajeev Rastogi, and Kyuseok Shim. 2000. Efficient algorithms for mining outliers from large data sets. In *Proceedings of the 2000 ACM SIGMOD International Conference on Management of Data*. Association for Computing Machinery, New York, NY, USA, 427–438. doi:10.1145/342009.335437
- [42] Shebati Rayana and Leman Akoglu. 2016. ODDS Library: Outlier Detection DataSets. <https://shebati.com/outlier-detection-datasets-odds/>.
- [43] Shebati Rayana, Wen Zhong, and Leman Akoglu. 2016. Sequential ensemble learning for outlier detection: A bias-variance perspective. In *2016 IEEE 16th international conference on data mining (ICDM)*. IEEE, 1167–1172.
- [44] Philipp Röchner, Simon Klüttermann, Franz Rothlauf, and Daniel Schläpfer. 2025. We Need to Rethink Benchmarking in Anomaly Detection. *arXiv:2507.15584* [cs.LG] <https://arxiv.org/abs/2507.15584>
- [45] Lukas Ruff, Robert Vandermeulen, Nico Goernitz, Lucas Deecke, Shoaib Ahmed Siddiqui, Alexander Binder, Emmanuel Müller, and Marius Kloft. 2018. Deep One-Class Classification. In *International Conference on Machine Learning*. 4393–4402.
- [46] David Salinas and Nick Erickson. 2024. TabRepo: A Large Scale Repository of Tabular Model Evaluations and its AutoML Applications. In *International Conference on Automated Machine Learning*. PMLR, 19–1.
- [47] Carl-Erik Särndal, Bengt Swensson, and Jan Wretman. 1992. *Model Assisted Survey Sampling*. Springer-Verlag. doi:10.1007/978-1-4612-4378-6
- [48] Bernhard Schölkopf. 2022. Causality for machine learning. In *Probabilistic and causal inference: The works of Judea Pearl*. 765–804.
- [49] Bernhard Schölkopf, Robert C Williamson, Alex Smola, John Shawe-Taylor, and John Platt. 1999. Support Vector Method for Novelty Detection. In *Advances in Neural Information Processing Systems*, S.olla, T. Leen, and K. Müller (Eds.), Vol. 12. MIT Press. https://proceedings.neurips.cc/paper_files/paper/1999/file/8725fb77f25776fa9076e44fcd776-Paper.pdf
- [50] Yuchen Shen, Haomin Wen, and Leman Akoglu. 2025. FoMo-0D: A Foundation Model for Zero-shot Tabular Outlier Detection. *Transactions on Machine Learning Research* (2025). <https://openreview.net/forum?id=XQZwpr9JE>
- [51] Tom Shenkar and Lior Wolf. 2022. Anomaly Detection for Tabular Data with Internal Contrastive Learning. In *International Conference on Learning Representations*. https://openreview.net/forum?id=_hszZbt46bT
- [52] M Sklar. 1959. Fonctions de répartition à n dimensions et leurs marges. In *Annales de l'ISUP*, Vol. 8. 229–231.
- [53] Jascha Sohl-Dickstein, Eric Weiss, Niru Maheswaranathan, and Surya Ganguli. 2015. Deep unsupervised learning using nonequilibrium thermodynamics. In *International conference on machine learning*. pmlr, 2256–2265.
- [54] Georg Steinbuss and Klemens Böhm. 2021. Benchmarking unsupervised outlier detection with realistic synthetic data. *ACM Transactions on Knowledge Discovery from Data (TKDD)* 15, 4 (2021), 1–20.

- [55] Hugo Thimonier, Fabrice Popineau, Arpad Rimmel, and Bich-Liên Doan. 2024. Beyond Individual Input for Deep Anomaly Detection on Tabular Data. In *Proceedings of the 41st International Conference on Machine Learning (Proceedings of Machine Learning Research, Vol. 235)*, Ruslan Salakhutdinov, Zico Kolter, Katherine Heller, Adrian Weller, Nuria Oliver, Jonathan Scarlett, and Felix Berkenkamp (Eds.). PMLR, 48097–48123. <https://proceedings.mlr.press/v235/thimonier24a.html>
- [56] Kai Ming Ting, Sunil Aryal, and Takashi Washio. 2018. Which Outlier Detector Should I use?. In *2018 IEEE International Conference on Data Mining (ICDM)*. 8–8. doi:10.1109/ICDM.2018.00015
- [57] Joaquin Vanschoren. 2018. Meta-Learning: A Survey. In *Automated Machine Learning*. <https://api.semanticscholar.org/CorpusID:52938664>
- [58] An Yang, Anfeng Li, Baosong Yang, Beichen Zhang, Binyuan Hui, Bo Zheng, Bowen Yu, Chang Gao, Chengen Huang, Chenxu Lv, Chujie Zheng, Dayiheng Liu, Fan Zhou, Fei Huang, Feng Hu, Hao Ge, Haoran Wei, Huan Lin, Jialong Tang, Jian Yang, Jianhong Tu, Jianwei Zhang, Jianxin Yang, Jiayi Yang, Jing Zhou, Jingren Zhou, Junyang Lin, Kai Dang, Keqin Bao, Kexin Yang, Le Yu, Lianghao Deng, Mei Li, Mingfeng Xue, Mingze Li, Pei Zhang, Peng Wang, Qin Zhu, Rui Men, Ruize Gao, Shixuan Liu, Shuang Luo, Tianhao Li, Tianyi Tang, Wenbiao Yin, Xingzhang Ren, Xinyu Wang, Xinyu Zhang, Xuancheng Ren, Yang Fan, Yang Su, Yichang Zhang, Yinger Zhang, Yu Wan, Yuqiong Liu, Zekun Wang, Zeyu Cui, Zhenru Zhang, Zhipeng Zhou, and Zihan Qiu. 2025. Qwen3 Technical Report. arXiv:2505.09388 [cs.CL] <https://arxiv.org/abs/2505.09388>
- [59] Jingkang Yang, Kaiyang Zhou, Yixuan Li, and Ziwei Liu. 2024. Generalized Out-of-Distribution Detection: A Survey. *International Journal of Computer Vision* 132, 12 (01 Dec 2024), 5635–5662. <https://doi.org/10.1007/s11263-024-02117-4>
- [60] Jaemin Yoo, Tiancheng Zhao, and Leman Akoglu. 2023. Data Augmentation is a Hyperparameter: Cherry-picked Self-Supervision for Unsupervised Anomaly Detection is Creating the Illusion of Success. *Trans. Mach. Learn. Res.* 2023 (2023).
- [61] Xiyuan Zhang, Danielle C. Maddix, Junming Yin, Nick Erickson, Abdul Fatir Ansari, Boran Han, Shuai Zhang, Leman Akoglu, Christos Faloutsos, Michael W. Mahoney, Cuixiong Hu, Huzefa Rangwala, George Karypis, and Bernie Wang. 2025. Mitra: Mixed Synthetic Priors for Enhancing Tabular Foundation Models. In *The Thirty-ninth Annual Conference on Neural Information Processing Systems*.
- [62] Xingxuan Zhang, Gang Ren, Han Yu, Hao Yuan, Hui Wang, Jiansheng Li, Jiayun Wu, Lang Mo, Li Mao, Mingchao Hao, et al. 2025. Limix: Unleashing structured-data modeling capability for generalist intelligence. *arXiv preprint arXiv:2509.03505* (2025).
- [63] Yue Zhao, Ryan Rossi, and Leman Akoglu. 2021. Automatic unsupervised outlier model selection. *Advances in Neural Information Processing Systems* 34 (2021), 4489–4502.
- [64] Yue Zhao, Sean Zhang, and Leman Akoglu. 2022. Toward unsupervised outlier model selection. In *2022 IEEE International Conference on Data Mining (ICDM)*. IEEE, 773–782.

Appendix

A ADBench Analyses

A.1 Summary Statistics

Table 3: ADBench datasets summary statistics

	Min	Max	Mean	Median
Samples	80	619,326	28,013	5,393
Features	3	1,555	371	512
Outlier fraction	0.03%	39.9%	10.0%	5.0%

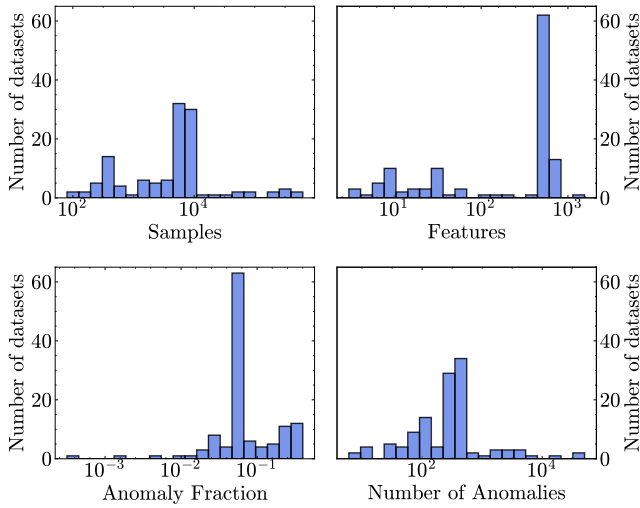


Figure 10: Summary statistics of ADBench datasets.

A.2 Demystifying ADBench: Details

A.2.1 Delving into DTE (Livernoche et al. [34]).

Background: Denoising Diffusion Probabilistic Models: A diffusion process describes a stochastic system in which the probability distribution evolves over time following the diffusion equation. Denoising diffusion probabilistic models [28, 53] consider the states corresponding to time steps $t > 0$ as latent variables. Let $\mathbf{x}_0 \sim q(\mathbf{x}_0)$ denote an observed data point sampled from the underlying data distribution and $\mathbf{x}_1, \dots, \mathbf{x}_T$ denote the corresponding latent variables. The **forward diffusion** process typically adds (Gaussian) noise at each time step according to a noise (variance) schedule β_1, \dots, β_T . Under Gaussian noise, the approximate posterior $q(\mathbf{x}_{1:T} | \mathbf{x}_0)$ is written as

$$q(\mathbf{x}_{1:T} | \mathbf{x}_0) := \prod_{t=1}^T q(\mathbf{x}_t | \mathbf{x}_{t-1}), \quad q(\mathbf{x}_t | \mathbf{x}_{t-1}) := \mathcal{N}(\mathbf{x}_t; \sqrt{1 - \beta_t} \mathbf{x}_{t-1}, \beta_t \mathbf{I}) \quad (2)$$

Using Gaussian distributions enables sampling \mathbf{x}_t in closed form at any time t as

$$q(\mathbf{x}_t | \mathbf{x}_0) := \mathcal{N}(\mathbf{x}_t; \sqrt{\bar{\alpha}_t} \mathbf{x}_0, (1 - \bar{\alpha}_t) \mathbf{I}), \quad (3)$$

where $\alpha_t := 1 - \beta_t$ and $\bar{\alpha}_t := \prod_{s=1}^t \alpha_s$.

Diffusion probabilistic models learn the reverse process transitions, a.k.a. the **backward denoising**. Starting at $p(\mathbf{x}_T) = \mathcal{N}(\mathbf{x}_T; 0, \mathbf{I})$, the joint distribution of the reverse process $p_\theta(\mathbf{x}_0 : T)$ decomposes into a product of terms

$$p_\theta(\mathbf{x}_{t-1} | \mathbf{x}_t) := \mathcal{N}(\mathbf{x}_{t-1}; \mu_\theta(\mathbf{x}_t, t), \Sigma_\theta(\mathbf{x}_t, t)) \quad (4)$$

After a finite sequence of transitions, the parameterized reverse process yields samples consistent with the data distribution.

Diffusion-based OD and DTE: Typical diffusion-based OD approaches take as input a timestep (as hyperparameter¹²) from which they simulate the reverse diffusion chain to generate the reconstruction. The distance between a data point and its denoised reconstruction is used as its anomaly score. Motivated by computationally expensive reverse diffusion, Livernoche et al. [34] embrace a simpler idea: **estimate the distribution over diffusion time**. In essence, the diffusion time serves as a surrogate for the distance from the data manifold, for which they derive an analytical formula under Gaussian noise.

In the following, we analyze DTE’s analytical form and its approximation in detail that establishes intriguing connections between denoising diffusion time, Gaussian noise variance and nearest neighbors. Consider $\mathbf{x}_s \in \mathbb{R}^d$, a given input point, to be the outcome of a forward diffusion process starting from the data manifold (i.e. an inlier). How can we estimate (the distribution over) its diffusion time, that is the number of forward steps (the larger, the more outlying)?

Assuming Gaussian noise as presented earlier in the Background, let $\sigma_t^2 = 1 - \bar{\alpha}_t$ denote the variance at time t . Given dataset \mathcal{D} sampled from the manifold, the posterior distribution over σ_t^2 can be written as

$$p(\sigma_t^2 | \mathbf{x}_s) \propto p(\mathbf{x}_s | \sigma_t^2) p(\sigma_t^2) = \sum_{\mathbf{x}_0} p(\mathbf{x}_s | \mathbf{x}_0, \sigma_t^2) p(\mathbf{x}_0) \quad (5)$$

$$= \sum_{\mathbf{x}_0 \in \mathcal{D}} \mathcal{N}(\mathbf{x}_s; \mathbf{x}_0, \sigma_t^2 \mathbf{I}) \propto \sigma_t^{-d} \sum_{\mathbf{x}_0 \in \mathcal{D}} \exp\left(-\frac{\|\mathbf{x}_s - \mathbf{x}_0\|^2}{2\sigma_t^2}\right) \quad (6)$$

$$\approx \sigma_t^{-d} \exp\left(-\frac{1}{\sigma_t^2} \min_{\mathbf{x}_0 \in \mathcal{D}} \frac{\|\mathbf{x}_s - \mathbf{x}_0\|^2}{2}\right). \quad (7)$$

The above approximation in Eq. (7) is obtained by employing exp and then log functions preceding the sum in the second term of Eq. (6), and approximating the resulting log-sum-exp term with the max function.

DTE and Gaussian Noise Outliers: The exact analytical posterior distribution, i.e. the first term in Eq. (6), can be interpreted as the sum of Gaussian distribution likelihoods, each centered on a data point $\mathbf{x}_0 \in \mathcal{D}$ with time-dependent variance. Effectively, DTE identifies data points as outliers if their probability is high(er) under a Gaussian distribution with a large(r) variance. This is a byproduct of diffusion with Gaussian noise. Starting from an inlier \mathbf{x}_0 on the data manifold, forward diffusion at time step t is equivalent to creating a sample drawn from a Gaussian centered on \mathbf{x}_0 and a variance that grows as a function of t . These are in essence simulated outliers; the larger the t , the more outlying.

In two variants of DTE, Livernoche et al. [34] train a deep neural network to directly predict t from \mathbf{x}_0 ; DTE-IG assumes t follows an Inverse Gamma distribution, while DTE-C categorizes t into

¹²Note that Livernoche et al. [34] show the sensitivity of diffusion-based OD algorithms to the choice of the starting timestamp hyperparameter in their Appendix A.

bins and simplifies the task as a classification one. To train such a network, they simulate noisy samples (i.e. outliers) from the given data points in \mathcal{D} using the forward diffusion process while varying t , the number of diffusion steps. They argue that, thanks to the space-filling property of diffusion, different regions of the feature space are sampled at different rates mimicking a variety of potential outliers. Notably, however, those **assumed outliers are limited to Gaussian noise with variance in the full d -dimensional feature space** as opposed to *sub*-spaces. (See Eq. (3) where covariance matrix is a scaled Identity matrix in $\mathbb{R}^{d \times d}$.)

DTE and k Nearest Neighbors:

The derivation of (7) uncovers an interesting connection between DTE and KNN: **the posterior over diffusion time is a function of the distance from a data point to its nearest neighbor in the dataset**. In practice, instead of the minimum squared distance to neighbors, DTE uses the average distance to k nearest neighbors (KNN) to better approximate the log-sum-exp especially for larger time steps. Then, their anomaly score, the mean of this posterior distribution, is proportional to

$$\frac{1}{K} \sum_{x_0 \in \text{KNN}(x_s)} \frac{\|x_s - x_0\|}{2}. \quad (8)$$

The approximate approach, coined as DTE-NP, employs a non-parametric (NP) estimation. As such, **DTE-NP produces a ranking (of data points by outlieriness) identical to that by average KNN distance**, a classical OD approach. Notably, the KNN algorithm by Ramaswamy et al. [41] is slightly different as it uses the largest, i.e. k th NN distance as the outlier score instead of the average. In fact, **KNN [41] is the second top algorithm reported on ADBench**, following DTE-NP. A deeper examination of DTE reveals why they perform similarly, despite appearing different.

A.2.2 Delving into FoMo-0D (Shen et al. [50]).

Next we analyze FoMo-0D [50] which performed competitively on ADBench, closely rivaling DTE (on average across hyperparameters) and KNN (2nd top performer). For easy reference, we present the comparison in Table 4, which reports the average rank based on AUROC across All (57) datasets, along with the p -values of the one-sided Wilcoxon signed rank test, comparing FoMo-0D to DTE-NP and KNN with author-recommended hyperparameter $k = 5$, and with **avg.** performance over varying HPs (denoted w/ superscript ^{avg}). We refer to the original paper for the details on these results.

Table 4: FoMo-0D vs. DTE-NP and KNN on ADBench, based on the average rank by AUROC across All (57) datasets and p -values of the one-sided Wilcoxon signed rank test.

	FoMo-0D	DTE-NP	KNN	DTE-NP ^{avg}	KNN ^{avg}
Rank(avg)	11.886	7.553	9.018	9.079	11.105
All	-	0.016	0.106	0.112	0.315
All \ {NLP, CV}	-	0.164	0.476	0.515	0.683
$d \leq 100$	-	0.415	0.700	0.752	0.860

The p -values on All (57) datasets suggest that FoMo-0D shows no statistically significant difference from the **second top** model KNN on ADBench at $p = 0.106$. Further, the differences vanish

when (the embedded, high-dimensional) NLP (i.e. text) and CV (i.e. image) datasets are excluded. In fact, over datasets with up to 100 dimensions, which aligns with FoMo-0D’s pretraining, the p -values become notably large. We also remark that FoMo-0D performs similarly to DTE-NP^{avg} and KNN^{avg}, where their expected performance is computed over various k values (as opposed to favorably chosen $k = 5$ in [34]) as suggested by the relatively larger ranks and p -values. Note that FoMo-0D is a foundation model that labels test points via a single forward pass given training points as context, requiring no hyperparameters to be tuned (nor any model to be trained from scratch).

Revisiting our original goal: *What makes FoMo-0D achieve as competitive results as these SOTA methods on ADBench, considering it was pretrained purely on synthetic datasets?* In fact, the astonishing performance of FoMo-0D on real-world datasets has been an unresolved question until the detailed analysis of DTE; in particular, the type of outliers it captures.

The key to the puzzle is the data prior from which the synthetic datasets used to pretrain FoMo-0D are drawn. Specifically, Gaussian mixture models (GMMs) with *diagonal* covariances are used to synthesize inliers, while the outliers are sampled from the same GMM with *inflated variances* in random sub-spaces, ensuring they lie outside the 90th percentile of the original GMM [50]. Overall, **FoMo-0D performs alike DTE (and by extension KNN) as it likewise models outliers as generated by Gaussian noise.**

B Proposed Benchmark Details

B.1 Real-World Benchmarks: OddBench and OvRBench

B.1.1 Keywords that indicate anomalousness: To test whether a feature value or a metadata is likely related to outlier detection, we check whether such a string contains one of the following words:

```
"fraud", "intrusion", "attack", "malware",
↪ "spam", "phishing", "defect", "failure",
↪ "fault", "error", "bug", "outlier",
↪ "anomaly", "abnormal", "irregular",
↪ "rare", "deviation", "exception",
↪ "deviation", "irregularity",
↪ "abnormality", "flaw", "disturbance",
↪ "variance", "misfire", "oddity",
↪ "discrepancy", "dissonance", "unusual",
↪ "quirk", "oddity", "peculiarity",
↪ "nonconformity", "misfit", "aberration",
↪ "mistake", "fault", "glitch", "hiccup",
↪ "error", "breakdown", "defect",
↪ "anomalies", "invalid", "vulnerabl",
↪ "breach", "exception", "fail",
↪ "critical", "extreme"
```

B.1.2 Duplicate Check. Tablib [17] contains a collection of all datasets from GitHub, without any duplication check. To solve this, we design a custom hashing function that is applied to each feature. When two datasets both contain a feature with the same hash value, we randomly drop one of these datasets. Our hashing function computes the average of five simple functions and considers two features equivalent if they share all five resulting values.

The five functions we use are $\sin(x)$, $\cos(e \cdot x)$, $\frac{x}{1+|x|}$, $\arctan(x)$, $\log(|x| + 1)$.

We design this hashing procedure so that dropping or shuffling features does not resolve potential hash conflicts. However, small variations (e.g., NaN imputation, Subset selection) still conceal hash conflicts. Thus, we also manually filter for duplicates.

B.1.3 Metadata. To improve the usability of OddBench, we add both feature names, a tablib identifier, and a link to the original dataset we processed to each dataset (when they are available). We also employ an LLM to generate short names for each dataset, and further let the LLM categorize the origin of each dataset into one of the following categories: "Engineering", "Science", "Logistics", "Human", or "Other", and add tags to the data that describe different scenarios. A word cloud of keywords generated by the same LLM is shown in Figure 4, while a distribution of tags is given in Figure 12.

The Large Language Model used here is (Qwen 3- 8B[58]). For each dataset it receives the following prompt:

```

1 I am trying to create anomaly detection datasets.
  For this, I parse the meta information of a large
  amount of tabular data and extract datasets that
  are suitable for anomaly detection. Now, given
  these datasets, I would like to expand each
  dataset slightly.
2 For this, I would like to have short, memorable,
  meaningful names for each dataset ("dataset\_name"
  ). Examples of these might be "PlanetaryMotion" ,
  "MonsterType" or "LifeExpectancy". So these names
  should be in CamelCase without spaces.
3 Additionally, I would like to have 5-10 keywords
  that describe the specific context of the dataset
  ("keywords"). Examples of keywords might be ["
  planets", "orbit", "gravity"] or ["monsters", "
  type", "strength", "weakness"].
4 Finally, I would also like to categorize the
  datasets by the domain they cover/ their origin ("
  origin"). Valid answers here are ["Logistics", "
  Engineering", "Science", "Human", "Other"]. Answer
  only with a single category out of these options.
5 Please answer in json format like this:
6 {
7   "reasoning": "Your reasoning here explaining why
  you chose these values",
8   "keywords": ["keyword1", "keyword2", "..."],
9   "dataset_name": "DatasetName",
10  "origin": "label_to_use",
11 }
12 Do not include anything else except this json
  object in your answer.

```

B.1.4 Finding representative sets. Finding the best representative set by minimizing Equation 1 requires evaluating $\binom{690}{50}$ different subsets. As it is thus infeasible to find the best representative set, we instead use an evolutionary algorithm to approximate it.

This evolutionary algorithm evaluates $1M$ different candidate sets S . In each step, it either randomly generates a subset (50% probability) or modifies a previously generated subset by switching one element for another random one (50% probability). We retain both the best- and worst-performing subsets (1% probability) to

improve the robustness of our optimization against local minima, but finally only report the best performing subset.

B.1.5 Sources of datasets used in OvRBench. We state the origin of each dataset from established tabular qualification benchmarks in OvRBench in Table 5.

Table 5: Number of datasets used for OvRBench excluding Tablib [17].

Data Source	Year	# Original	# Used
OpenML-CC18 [5]	2017	72	1
AutoML [23]	2019	39	0
TabZilla [36]	2023	36	3
Talent-CLS [33]	2024	180	52
TabRepo [46]	2024	246	95
BCCO-CLS [62]	2025	106	28
TabArena [21]	2025	37	22
Total	-	716	201

Note that datasets can overlap between different data sources. If a dataset (by dataset name) appears in multiple benchmarks, we keep only the version from the newest source.

B.1.6 Analysis of OddBench and OvRBench. This section assesses the characteristics and performance baselines of the proposed real-world benchmarks.

Figure 11 demonstrates that both OddBench and OvRBench encompass a wide range of different dataset characteristics. These characteristics are both semantic and statistical (Figure 12), ensuring the suitability of our benchmarks across a wide range of outlier detection applications.

Further, we evaluate the performance of the best one-class algorithm of our study (OUTFORMER, see Sec. 4) against a simple supervised baseline (a random forest [7]) in Figure 13. Despite the theoretical advantage of one-class methods in low-anomaly regimes (Figure 1), the random forest still consistently outperforms the one-class approach. This performance gap highlights a significant deficiency in current outlier detection methods and positions our benchmarks as critical tools for guiding future algorithmic advancements.

B.2 Synthetic Benchmark: SynBench

We simulate 800 datasets spanning five outlier categories (GMM, SCM-Measurement, SCM-Structural, Copula-Probabilistic, and Copula-Dependence) with 160 datasets per category. Within each category, we diversify both inlier and outlier distributions by sampling feature dimensions from $[2,100]$, outlier ratios from 5% to 15%, and dataset sizes between 1,000 and 6,000 samples.

B.2.1 Gaussian Mixtures.

Inliers. We simulate inliers by sampling from multivariate Gaussian mixture models (GMMs) with varying numbers of components and dimensions. Each dataset is generated from an m -component GMM in d dimensions, where component means $\mu^{(k)} \in [-5, 5]^d$ and diagonal covariances $\Sigma_{jj}^{(k)} \in (0, 5]$ for all $k \in [m]$

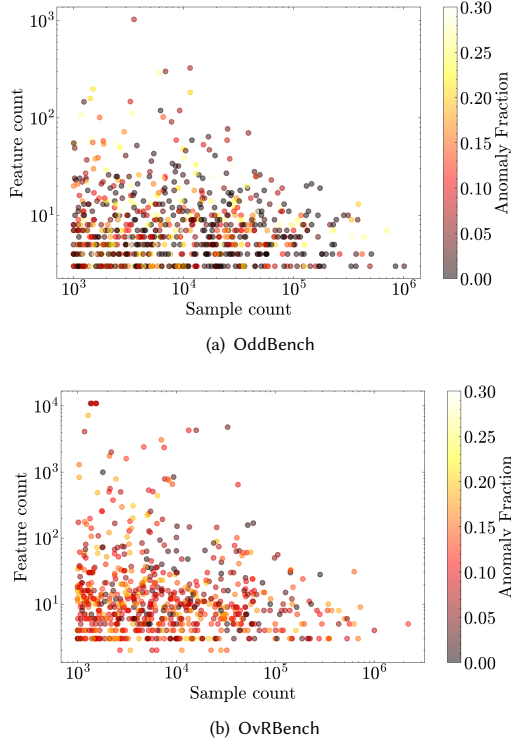


Figure 11: Dataset statistics of (a) OddBench and (b) OvRBench, showing a high range of anomaly detection settings.

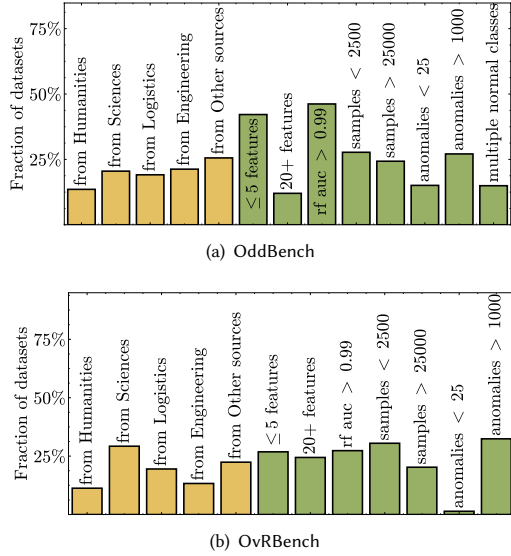


Figure 12: Dataset origin (yellow) and situational tags (green) of (a) OddBench and (b) OvRBench, enabling specialized research for many different settings.

and $j \in [d]$. For each dataset, we sample m and d uniformly, with up to $M = 5$ mixture components and $D = 100$ dimensions. To increase diversity, we apply a linear transformation $T(\mathbf{x}) = \mathbf{W}\mathbf{x} + \mathbf{b}$, where $\mathbf{W} \in \mathbb{R}^{d \times d}$ and $\mathbf{b} \in \mathbb{R}^d$ have entries independently drawn

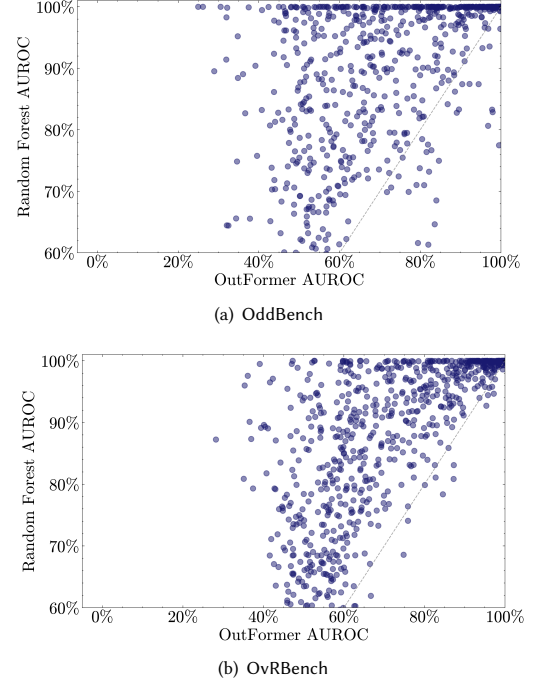


Figure 13: Random Forest (supervised classification) performance versus OutFormer (one-class outlier detection) performance on (a) OddBench and (b) OvRBench show the high potential for improvement of unsupervised methods that our benchmarks allow.

from $\text{Unif}[-1, 1]$. This transformation induces a new GMM with transformed means $T(\boldsymbol{\mu}^{(k)}) = \mathbf{W}\boldsymbol{\mu}^{(k)} + \mathbf{b}$ and full (non-diagonal) covariances $T(\boldsymbol{\Sigma}^{(k)}) = \mathbf{W}\boldsymbol{\Sigma}^{(k)}\mathbf{W}^\top, \forall k \in [m]$.

Outliers. We generate *contextual subspace outliers* by first randomly selecting a GMM component k and a subset of dimensions $\mathcal{S} \subseteq [d]$. We then inflate the variances of the selected component along the chosen subspace by scaling the diagonal entries as $s \sum_{jj}^{(k)}$ for all $j \in \mathcal{S}$, while keeping the component mean unchanged. Samples are drawn from this variance-inflated GMM, and points are labeled as outliers if their Mahalanobis distance exceeds the 90th percentile of the original (uninflated) GMM. The severity of the generated outliers is controlled by the subspace fraction $|\mathcal{S}| = \alpha d$ and the inflation factor s , which govern the dimensional extent and magnitude of the perturbation, respectively. Table 6 provides the range of hyperparameter configurations for sampling datasets from the GMM prior.

B.2.2 Structural Causal Models.

Inliers. Structural causal models (SCMs) characterize data-generating processes by explicitly modeling causal dependencies via directed acyclic graphs (DAGs) and structural equations. Formally, an SCM is defined by a graph $G = (V, E)$, where each node $j \in V$ represents a variable governed by the structural equation $X_j = f_j(X_{\text{Pa}(X_j; G)}, \epsilon_j)$, with $\text{Pa}(X_j; G)$ denoting the set of parent variables of X_j in G , and ϵ_j capturing exogenous noise. To generate SCM inliers, we first

Table 6: Hyperparameters for Gaussian Mixture Model (GMM) Data Prior

Hyperparameter	Values	Description
m	[1, 5]	Number of mixture components
d	[2, 100]	Dimensionality of data
$\mu_j^{(k)}$	[-5, 5]	Component means
$\Sigma_{jj}^{(k)}$	(0, 5]	Diagonal variances
α	$[\frac{1}{d}, 1]$	Fraction of dimensions for variance inflation
s	[5, 10]	Variance inflation factor for subspace outliers
r	[0.02, 0.2]	Outlier rate of contamination

instantiate the causal graph G using a multilayer perceptron (MLP). Sparsity is induced by applying a binary weight mask with a ratio sampled from (0.4, 0.6), yielding a sparse dependency structure over a selected set of d nodes and producing d -dimensional observations. Nonlinear causal mechanisms are modeled via an activation function $a(\cdot)$. After initialization, the MLP weights are frozen to simulate a fixed causal mechanism. Inlier samples are generated by forward-propagating through the MLP and subsequently flattened into multi-dimensional feature vectors.

Measurement Outliers. To generate measurement outliers, we randomly select a variable $X_j \in \mathcal{X}$ and resample its exogenous noise as $\epsilon_j \sim \mathcal{N}(0, s)$, thereby inflating its variance by s . The induced perturbation is then propagated to all descendant variables through the fixed structural equations, producing a multivariate outlier. This process models exogenous shocks while preserving the underlying causal structure and mechanisms. For each SCM, outliers are generated by applying this procedure to a random fraction r of the nodes.

Structural Outliers. Structural outliers arise from changes in the underlying causal mechanisms. We generate such outliers by intervening on the MLP-based SCM, either by *breaking* a causal edge (setting its weight to zero) or by *reversing* its direction (multiplying the weight by -1). These interventions modify parent-child relationships and thus alter the data-generating process. We apply edge perturbations with total probability 0.2 (split evenly between breaking and reversing) and enforce a filtering criterion that ensures at least one leaf node is affected. Figure 14 provides an example of generated SCMs, and Table 7 provides the hyperparameter settings of the SCM priors.

B.2.3 Copulas.

Inliers. Real-world univariate features often exhibit skewed, heavy-tailed distributions [12]. Although SCMs yield non-Gaussian marginals, they do not offer explicit control over feature-wise distributions; we therefore employ copula models [31, 37]. By Sklar’s theorem [52], any joint CDF of continuous variables $\{X_j\}_{j=1}^d$ with marginals $\{F_j\}$ can be written as $F(x_1, \dots, x_d) = C(F_1(x_1), \dots, F_d(x_d))$, allowing the marginal distributions and dependence structure to be specified independently. We draw each marginal from a diverse set of parametric families (Gaussian, Beta, Exponential, Student’s t , Power-law, and Log-logistic) and model dependence using either a Gaussian or (bivariate) vine copula. Inliers are generated by sampling $\mathbf{u} \sim C$ on $[0, 1]^d$ and applying the inverse transforms $x_j = F_j^{-1}(u_j)$. By

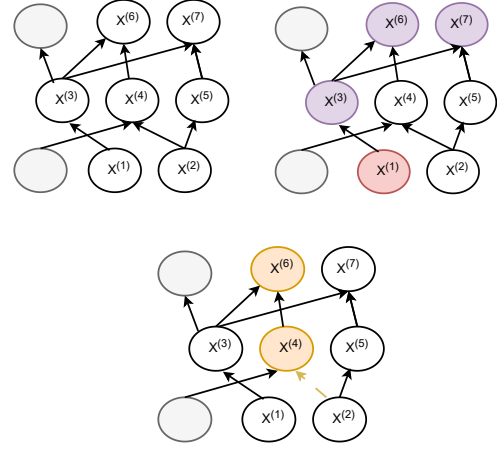


Figure 14: (Top-Left): We construct an SCM and select a subset of seven nodes, from which 7-dimensional inlier samples are generated under a frozen causal structure. **(Top-Right):** Measurement outliers are produced by inflating the variance of node $x^{(1)}$, causing the perturbation to propagate to $x^{(3)}$, $x^{(6)}$, and $x^{(7)}$. **(Bottom):** Structural outliers are generated by breaking the causal link between $x^{(2)}$ and $x^{(4)}$, thereby altering the dependency node $x^{(6)}$.

varying both the marginals and the copula, we synthesize a wide range of realistic tabular inlier distributions.

Probabilistic Outliers. To generate probabilistic outliers, we randomly select a subset of features and perturb their copula coordinates by shifting them toward the boundaries, replacing u_j with small values $u_{\text{perturb}} \in [0.1, 0.3]$ or large values $u_{\text{perturb}} \in [0.7, 0.9]$. The perturbation is applied to a fraction $\gamma_{\text{perturb}} \in [0.02, 0.2]$ of the dimensions, with the constraint that at least one feature is always perturbed.

Dependence Outliers. To generate dependence outliers, we alter the copula coordinates to break the original dependence structure, either by inverting selected dimensions (i.e., $u_j \leftarrow 1 - u_j$) or by randomly permuting them. The number of perturbed dimensions is sampled as $k_{\text{invcorr}} \in \left[\left\lceil 1 + \frac{d}{3} \right\rceil, \min \left(\left\lceil 1 + \frac{2d}{3} \right\rceil, d \right) \right]$, corresponding to approximately 33%–67% of the total dimensions. Table 8 provides the hyperparameter settings of the Copula priors.

Table 7: Hyperparameters for Structural Causal Model (SCM) based Data Priors

Hyperparameter	Values	Description
MLP depth	[3, 5]	Number of layers used to generate the DAG
MLP width	[20, 40]	Number of nodes per layer
Edge-drop rate	[0.4, 0.6]	Fraction of edges randomly removed to form the DAG
d	[2, 100]	Number of selected nodes as features \mathcal{X}
$a(\cdot)$	{ReLU, tanh, sigmoid}	Activation function for structural equations
s	[5, 10]	Variance inflation factor for measurement outliers
p^{break}	[0.1]	Probability of removing a causal edge for structural outliers
p^{flip}	[0.1]	Probability of reversing a causal edge for structural outliers
r	[0.02, 0.2]	Outlier rate of contamination

Table 8: Hyperparameters for Copula Data Prior

Hyperparameter	Values	Description
d	[2, 100]	Number of features / copula dimension
C	{Gaussian, Vine (bivariate)}	Copula parameter family
α_{indp}	[0.1, 0.3]	Fraction of features set independent in copula
Bivariate vine	Gauss., Stu., Clayton, Gumbel, Frank, Joe	Bivariate family for each Vine edge
Marginal	{Gauss., Beta, Exp., Stu. t, Power-law, Log-logistic}	Marginal family for each feature
μ/σ	(-1, 1)/(0.5, 1.0)	mean/variance for Gaussian
a/b	(1, 5)/(1, 5)	for Beta
$loc, scale$	-5, 10	Variables rescaled as $loc + scale \times x_{\text{beta}}$ for effective range [-5, 5]
λ / loc	(0.5, 1.0), -5	Exponential distribution scale / shift as $loc + x_{\text{exp}}$ for effective range
df	(3, 10)	Degrees of freedom for Student's t
$loc, scale$	[-1, 1], [0.5, 1.0]	Variables rescaled as $loc + scale \times x_{\text{stu}}$ for effective range
$a / loc \ \& \ scale$	(0.5, 5) / -5 & 5	Power law exponent, location & scale for effective range
$c / loc \ \& \ scale$	(0.5, 5) / -5 & 5	Log-logistic shape, location & scale for effective range
γ_{perturb}	[0.02, 0.2]	Fraction of dimensions to perturb for probabilistic outliers
u_{perturb}	[0.1, 0.3] or [0.7, 0.9]	CDF perturbation for probabilistic outliers
Copula perturbation	{inverse_corr, random_permutation}	Types of dependence outliers
k_{invcorr}	[1, 67]	Num of dimensions to invert for dependence outliers

C Experiment Setup Details

C.1 Selected Baselines and HP Configurations

Table 9 gives an overview of the benchmark OD baselines. Below we briefly describe each of the baselines and our training/evaluation configurations, with a detailed list of HPs in Table 10.

OCSVM. [49] learns a decision boundary by maximizing the margin between the origin and the normal data, effectively enclosing the region of high data density. The kernel (linear vs. RBF) controls whether this boundary is linear or nonlinear, ν specifies an upper bound on the fraction of outliers (and a lower bound on support vectors), and γ (RBF only) determines the smoothness of the boundary, with larger values yielding more localized, complex decision surfaces.

KNN. [41] assigns an anomaly score to each instance based on its distance to the k -th nearest neighbor, with larger distances indicating greater anomaly likelihood.

LOF. [8] measures the degree of anomaly of a sample by comparing its local density to that of its neighbors. The hyperparameter $N_{\text{neighbors}}$ specifies the size of the local neighborhood used for density estimation, where smaller values focus on finer local structure and larger values capture broader neighborhood trends.

CBLOF. [27] computes anomaly scores by first clustering the data and then measuring each sample's distance to large, dense clusters. The hyperparameter N_{clusters} controls the clustering granularity, while α and β define the criteria for separating large and small clusters, thereby modulating the anomaly score assigned to samples in small clusters.

IForest. [32] isolates anomalies by recursively partitioning the data using random feature selection and random split values. The hyperparameter $N_{\text{estimators}}$ specifies the number of trees in the ensemble, improving stability with larger values, while max_samples controls the subsample size used to build each tree, affecting both detection sensitivity and computational cost.

EGMM. [24] scores anomalies by averaging the log-likelihoods assigned to each sample across a retained ensemble of Gaussian mixture models, where lower likelihood indicates higher anomaly. Models with poor out-of-bag likelihood are pruned using a `discard` threshold, and the hyperparameter k controls the number of mixture components in each GMM. Since EGMM is computationally expensive due to repeated GMM fitting, for large datasets in Odd-Bench and OvrBench we cap the context length at 50,000 and restrict the number of features to at most 200.

GOAD. [4] trains a classifier to distinguish among many random linear transformations of normal data—where N_{rots} is the number of such transformations, m is the margin enforcing separation in the transformation-consistency loss, and λ balances that loss against cross-entropy. At test time, samples that fail to produce transformation-discriminative embeddings (i.e., lie far from learned transformation clusters) are scored as anomalous.

ICL. [51] learns anomaly-sensitive representations via contrastive learning by distinguishing genuine feature relationships from corrupted (negative) samples, with anomalies yielding higher contrastive loss. Key hyperparameters include the temperature τ , which controls the sharpness of the contrastive objective, and the number of negative samples, which governs discrimination strength. The window size k defines the number of neighboring samples used to form the local context; since varying k can trigger out-of-memory errors on large datasets, we retain the default setting.

DTE-C & DTE-NP. [34] are diffusion-based anomaly detection methods that score anomalies via reconstruction error under a learned diffusion process, with DTE-NP modeling continuous data non-parametrically and DTE-C extending the framework to categorical features via discrete diffusion. In DTE-NP, k controls the neighborhood size used for local density estimation during scoring. DTE-C extends diffusion-based anomaly detection to categorical data, where $N_{\text{categories}}$ determines the discrete state space modeled by the diffusion process, and the diffusion timestep controls the noise schedule length.

NPT-AD. [55] is a deep anomaly detection method for tabular data that leverages Non-Parametric Transformers (NPTs) to jointly model both feature–feature and sample–sample dependencies. In a reconstruction framework, an NPT is trained to reconstruct masked features of normal samples using the entire training set non-parametrically, and at inference the model’s ability (or failure) to reconstruct masked portions yields an anomaly score, with larger reconstruction errors indicating anomalies. Following [55], we adopt the same learning schedule and train the model for 2000–4000 steps. For small datasets, we vary r , the number of features masked simultaneously, in $\{1, 2, 3, 4\}$, while for large datasets we fix $r = 1$ due to computational constraints. Since large m (the number of masking patterns) leads to prohibitive inference cost, we keep m small. To fit memory limits, we subsample training data to at most 50,000 instances and 150 features for large datasets, and batch test-time evaluations accordingly.

FoMo-0D. [50] is a foundation model specifically trained of OD tasks. Due to context length and feature dimension limitation, during inference on all benchmarks, we will take up to 5,000 inlier points as contexts and sub-sample 100 dimensions randomly if the dataset has more than 100 dimension.

TabPFN-OD. TabPFN-OD repurposes TabPFN [30] for outlier detection using a feature-wise self-prediction scheme. Given normal training data $\mathbf{x}_{\text{train}} \in \mathbb{R}^d$ and test data \mathbf{x}_{test} , we randomly select a subset of features and, for each feature j , train a TabPFN regressor to predict x_j from \mathbf{x}_{-j} using only normal samples; anomaly scores are computed as the average absolute prediction error across selected features. This method leverages inter-feature dependencies

in normal data, which anomalies tend to violate. For large datasets we sample up to 100 features and fix the context length to 5000.

OUTFORMER. [13] is a recent foundation model that improves over FoMo-0D, by training with mixed priors and self-evolving curriculum learning. Following the paper, we use up to 1,000 inlier points and sub-sample 100 dimensions randomly, ensembling across 50 forward runs.

C.1.1 Training Details. For shallow, deep, and foundation models, all experiments are conducted on six NVIDIA A6000 GPUs with AMD EPYC 7742 64-core processors. For shallow methods, we exhaustively evaluate all hyperparameter (HP) configurations and report performance for each setting. In contrast, deep models typically involve much larger HP spaces and substantially longer training times; therefore, we randomly sample five HP configurations from Table 10 to evaluate their performance.

C.2 Performance Metrics and Statistical Tests

C.2.1 Ranking Based Metrics. For ranking and group based metrics, we adopt 5 metrics following the previous FM literature [61] and give a brief introduction of the metrics.

Average Rank. Let \mathcal{M} be the set of models and \mathcal{D} the set of evaluation datasets. For each model $m \in \mathcal{M}$ and dataset $\delta \in \mathcal{D}$, let $\text{rank}_{\delta}(m)$ denote the performance rank of m on δ , with smaller values indicating better performance. The average rank of model m is defined as

$$\text{AvgRank}(m) = \frac{1}{|\mathcal{D}|} \sum_{\delta \in \mathcal{D}} \text{rank}_{\delta}(m). \quad (9)$$

Elo Rating. Elo rating aggregates pairwise win-loss outcomes into a global ranking by treating each model as a player [18]. For each dataset, models are compared in a round-robin manner, with match outcomes determined by relative performance and ties allowed within a tolerance. Ratings are updated using the standard Elo scheme with initial rating $R_0 = 1000$, K-factor $K = 32$, and tie threshold $\epsilon = 0.5$, yielding final scores that reflect a model’s relative strength across all datasets.

Winrate. Winrate quantifies the fraction of pairwise comparisons in which a model outperforms others across datasets. For a model $m \in \mathcal{M}$, it is defined as

$$\text{Winrate}(m) = \frac{1}{|\mathcal{D}|(|\mathcal{M}| - 1)} \sum_{\delta \in \mathcal{D}} \sum_{\substack{m' \in \mathcal{M} \\ m' \neq m}} \left(\mathbb{I}[E_{\delta}(m) < E_{\delta}(m')] + \frac{1}{2} \mathbb{I}[E_{\delta}(m) = E_{\delta}(m')] \right), \quad (10)$$

where E denotes an error metric (e.g., $E = 1 - \text{AUROC}$), $\mathbb{I}[\cdot]$ is the indicator function, and ties contribute half a win. Although defined using AUROC, this metric applies to other performance measures such as AUPRC.

Rescaled AUC (rAUC). rAUC mitigates differences in dataset difficulty by normalization of model errors within each dataset relative to the best and worst performers. For dataset δ , the rescaled AUC of model m is defined as

$$\text{rAUC}_{\delta}(m) = 1 - \frac{E_{\delta}(m) - \min_m E_{\delta}(m)}{\max_m E_{\delta}(m) - \min_m E_{\delta}(m)}. \quad (11)$$

Table 9: Overview of benchmarked OD baselines on MACRODATA, listed chronologically, which are selected from Top-2 methods across various survey and benchmarking studies as cited in column 5.

Method	Abbrev.	Year	Type	Top-2 in:	Code	Usage
One-class Support Vector Machine [49]	OCSVM	1999	Shallow	[16]	PyOD	One Class
K-th Nearest Neighbors [41]	KNN	2000	Shallow	[9, 25, 50, 55]	PyOD	Un- & One Class
Local Outlier Factor [8]	LOF	2000	Shallow	[9, 19, 25]	PyOD	Un- & One Class
Clustering Based Local Outlier Factor [27]	CBLOF	2003	Shallow	[26]	PyOD	Un- & One Class
Isolation Forest [32]	IForest	2008	Shallow	[16, 19, 20, 26]	PyOD	Un- & One Class
Ensemble Gaussian Mixture Model [24]	EGMM	2013	Shallow	[20]	Ours	Un- & One Class
Classification Based AD using General Data [4]	GOAD	2020	Deep	[51]	Paper	Un- & One Class
Internal Contrastive Learning [51]	ICL	2022	Deep	[50, 51]	Paper	One Class
Prior-data Fitted Network [30]	TabPFN-OD	2022	Foundation	-	Paper+Ours	One Class
Non-Parametric Transformers for AD [55]	NPT-AD	2023	Deep	[55]	Paper	One Class
Diffusion Time Estimation (Non Parametric) [34]	DTE-NP	2024	Shallow	[34, 50]	Paper	Un- & One Class
Diffusion Time Estimation (Categorical) [34]	DTE-C	2024	Deep	[34]	Paper	One Class
Zero-shot Tabular Outlier Detection [50]	FoMo-0D	2025	Foundation	[50]	Paper	One Class
Mixed Prior Tabular Outlier Detection [13]	OUTFORMER	2026	Foundation	[13]	Paper	One Class

The rAUC is calculated by averaging $\text{rAUC}_\delta(m)$ across all datasets.

Champion Delta. Let $m^* = \arg \min_m E(m)$ denote the best-performing (champion) model. The Champion Delta of model m is defined as

$$\text{CD}(m) = \left(1 - \frac{E(m^*)}{E(m)}\right) \times 100, \quad (12)$$

measuring the relative percentage performance gap between model m and the champion.

C.2.2 Statistical Tests.

Permutation Test. Given two models evaluated on the same datasets, we compute per-dataset performance differences $d_i = s_i^{(A)} - s_i^{(B)}$ and discard ties. The test statistic is $T = \sum_i d_i$, and under the null hypothesis of equal performance, randomly flipping the signs of d_i yields a reference distribution

$$T^{(b)} = \sum_i \epsilon_i d_i, \quad \epsilon_i \in \{-1, +1\}.$$

The one-sided p -value is estimated as $p = \Pr(T^{(b)} \geq T)$, quantifying the probability that model A outperforms model B by chance; unlike a sign test, this permutation test accounts for the magnitude of performance differences. Compared to the Wilcoxon signed-rank test, this permutation test makes fewer distributional assumptions and directly models the null hypothesis via random sign flips of observed differences. It is particularly well-suited for benchmark comparisons with heterogeneous effect magnitudes, where Wilcoxon’s ranking can discard meaningful scale information.

A value ≥ 0.95 indicates that the column model wins significantly, while a value ≤ 0.05 indicates that the row model wins significantly; values in between imply no statistically significant difference. In general, smaller values provide stronger evidence in favor of the row model, whereas values close to 0.5 indicate essentially no difference between the two models.

D Additional Results

We provide additional results on individual benchmark’s AUPRC and AUROC performances, with time analysis shown in Figure 23.

D.1 AUPRC Results on Individual Benchmarks

Table 11 and Figure 15 show the performance comparison and pairwise permutation test results w.r.t. AUPRC on OddBench. The results underscore the effectiveness of foundation models for OD (see the last three rows): OUTFORMER outperforms all baselines with all $p \leq 0.05$. TABPFN-OD and FoMo-0D follow with similar results, outperforming all shallow and deep baselines, except EGMM. Notably, deep models do not achieve competitive performance mainly due to their hyperparameter (HP) sensitivity as we present in the following (Recall that results are based on average performance across HP configurations). EGMM and DTE-NP stand out as competitive shallow (classical) methods.

Table 12 and Figure 16 show the performance comparison and pairwise permutation test results on OvRBench. EGMM followed by DTE-NP stand out as two competitive classical methods, and outperform FoMo-0D significantly. All foundation models are competitive overall, with OUTFORMER outperforming all baselines ($p \leq 0.05$) except EGMM ($p = 0.255$). These results on our two large-scale real-world benchmarks OddBench and OvRBench highlight the prowess of foundation models for OD.

Finally, Table 13 and Figure 17 show the results on our simulated datasets in SynBench, with similar findings.

D.2 AUROC Results Combined and on Individual Benchmarks

Table 14 and Figure 18 present the AUROC performance and permutation test results on OddBench. OUTFORMER and DTE-NP achieve the strongest overall performance, with foundation models generally offering the leading edge. Among shallow methods, DTE-NP emerges as the strongest performer, followed by EGMM and KNN. Deep models generally underperform, mainly due to their hyperparameter sensitivity. Foundation models OUTFORMER and TABPFN-OD achieve strong performance, both outperforming all other baselines significantly ($p < 0.05$), except DTE-NP ($p = 0.583$ against OUTFORMER, and $p = 0.772$ against TABPFN-OD).

Table 10: Hyperparameter configurations for the baselines.

Model	List of Possible HPs	#Models
OCSVM	kernel: [rbf , linear] v: [0.05, 0.2, 0.5 , 0.8] γ : [scale , 0.1, 1.0] (rbf only)	16
KNN	k: [5 , 10, 20, 50, 100]	5
LOF	$N_{\text{neighbors}}$: [10 , 20 , 50, 100]	4
CBLOF	N_{clusters} : [4, 8 , 16, 32] α : [1, 0.5, 0.9 , 1] β : [2, 5 , 10]	48
IForest	$N_{\text{estimators}}$: [50, 100 , 200] max_samples: [64, 128, 256]	9
EGMM	k : [(1,2,3,4,5), (6,7,8,9,10)] $N_{\text{bootstrap}}$ [5, 15] Discard threshold: [0.85]	4
GOAD	m : [0.5, 1], λ : [0.1 , 0.5] N_{rots} : [128, 256 , 512] Embedding dimension: [32 , 64] MLP layers: [2, 3], Leaky ReLU: [0.1 , 0.2] Epochs: [1, 5, 10], Batch size: 64, LR: 0.001, Optimizer: Adam	288
ICL	Window_size $k \in \{2, 10, d - 150\}$ (dimension-based) Embed_dim: [200 , 100] Loss_temperature r : [0.1 , 0.5] F/G-network layers: [2,3], BatchNorm Num_negatives: [100, 1000] Num_epochs: [500, 2000], Lr = [1e-3 , 1e-4] Activation: LeakyReLU [0.1, 0.2], Optimizer: Adam	128
NPT-AD	r : [1, 2, 3, 4] (dataset specific) Embed_dim e : [16, 32] m : [1, 2, 4], p_{mask} = [0.15, 0.25] Num_transformer blocks: [2, 4] Num_steps: [2000, 4000] Batch_size: 32, LR: 1e-3 Optimizer: LAMB(0.9, 0.999) with Lookahead	192
DTE-NP	k: [5 , 10, 20, 50, 100]	5
DTE-C	$N_{\text{categories}}$: [5, 7, 10] Diffusion_timestep: [100, 300 , 500] Hidden_layers: [{ 256, 512, 256 }, {256, 256}] Dropout: [0.3, 0.5] Activation: ReLU Epochs: [350, 400], Lr: 1e-4	72

Table 15 and Figure 19 report the corresponding AUROC results on OvRBench, where the shallow methods KNN, EGMM, and DTE-NP, as well as the foundation models OUTFORMER and TABPFN-OD achieve the strongest overall results, significantly outperforming the rest of the baselines while being comparable among themselves.

Table 16 and Figure 20 report AUROC performance comparison on SynBench. OUTFORMER, TABPFN-OD and EGMM achieve strong results, significantly outperforming the rest of the baselines, where OUTFORMER outperforms all baselines significantly ($p < 0.05$).

Table 17 and Figure 21 summarize AUROC performance across all 2,446 datasets. OUTFORMER and TABPFN-OD achieve strong results, where OUTFORMER outperforms all baselines significantly ($p < 0.05$) - establishing FM as the dominant approach to OD.

D.3 HP Sensitivity Analysis

Figure 22 illustrates the inter-quartile range of performance variations induced by different hyperparameter configurations, highlighting each method’s sensitivity to hyperparameter (HP) choices. Among shallow models, ensemble based IForest and EGMM exhibit relatively strong HP robustness. In contrast, deep models are generally more sensitive to HP settings, due to the large hyperparameter spaces introduced by architectural design, optimization and regularization.

Foundation models (FMs) fully mitigate this issue by adopting a unified “one-model-for-all” paradigm, eliminating the need for per-task hyperparameter selection. Combined with low-latency inference, this makes FMs truly plug-and-play for practical deployment.

Table 11: Overall AUPRC performance comparison across models on the public partition of OddBench (690 datasets). Colors depict OD method categories, where green, blue, and red respectively denote shallow (classical), deep, and foundation models. Best results of each category are shown in bold, while global best is underlined. OUTFORMER achieves the strongest overall performance, underscoring the effectiveness of foundation models.

	Model	Avg. Rank (\downarrow)	ELO (\uparrow)	Winrate (\uparrow)	rAUC (\uparrow)	C_{Δ} (\downarrow)
Shallow	OCSVM	6.42 \pm 2.8	1180	0.57	0.694 \pm 0.26	0.35
	KNN	6.76 \pm 3.3	861	0.53	0.684 \pm 0.28	0.31
	LOF	6.86 \pm 3.9	915	0.53	0.676 \pm 0.28	0.33
	CBLOF	7.98 \pm 3.6	786	0.44	0.632 \pm 0.30	0.35
	IForest	8.43 \pm 4.1	1072	0.43	0.589 \pm 0.31	0.39
	EGMM	5.83 \pm 4.1	1135	0.60	0.724 \pm 0.30	0.25
	DTE-NP	5.91 \pm 3.3	1018	0.60	0.710 \pm 0.28	0.30
Deep	GOAD	10.98 \pm 3.6	741	0.22	0.483 \pm 0.29	0.41
	ICL	8.10 \pm 3.7	1105	0.44	0.642 \pm 0.28	0.36
	DTE-C	7.64 \pm 3.8	1199	0.47	0.651 \pm 0.29	0.33
	NPT-AD	10.38 \pm 4.1	671	0.27	0.502 \pm 0.31	0.40
FM	TabPFN-OD	6.12 \pm 4.0	929	0.58	0.716 \pm 0.29	0.26
	FoMo-OD	6.51 \pm 4.4	<u>1207</u>	0.56	0.721 \pm 0.29	0.25
	OutFormer	<u>5.43</u> \pm 3.9	1180	<u>0.63</u>	<u>0.739</u> \pm 0.28	<u>0.23</u>

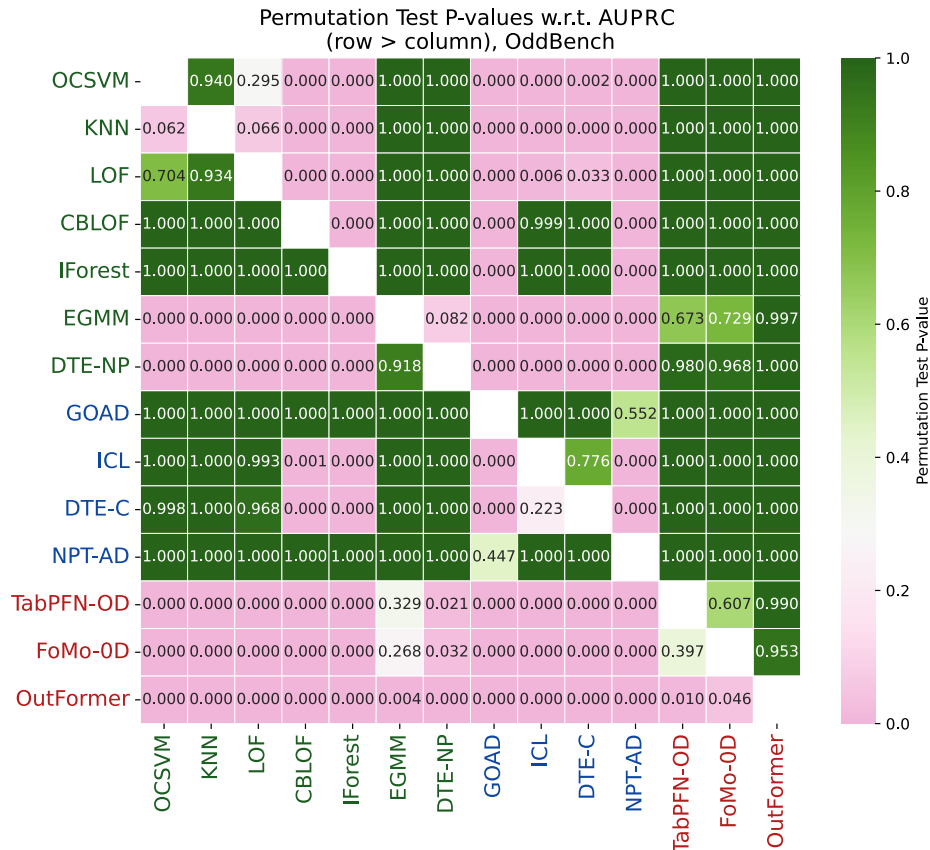


Figure 15: Paired permutation test results w.r.t. AUPRC across 690 public OddBench datasets. All foundation models achieve strong performance (last three rows), with OUTFORMER outperforming all baselines significantly ($p \leq 0.05$). EGMM and DTE-NP emerge as the best-performing shallow methods, while deep models do not achieve competitive results, mainly due to hyperparameter sensitivity.

Table 12: Overall AUPRC performance comparison across models on the public partition of OvRBench (756 datasets). Colors depict OD method categories, where green, blue, and red respectively denote shallow (classical), deep, and foundation models. Best results of each category are shown in bold, while global best is underlined. EGMM and OUTFORMER achieve the strongest overall results, significantly outperforming the rest of the baselines.

	Model	Avg. Rank (\downarrow)	ELO (\uparrow)	Winrate (\uparrow)	rAUC (\uparrow)	C_{Δ} (\downarrow)
Shallow	OCSVM	6.97 \pm 2.9	1127	0.53	0.791 \pm 0.18	0.30
	KNN	6.51 \pm 3.4	1254	0.56	0.805 \pm 0.20	0.26
	LOF	6.97 \pm 3.9	1062	0.53	0.775 \pm 0.21	0.28
	CBLOF	7.83 \pm 3.7	1221	0.47	0.758 \pm 0.23	0.31
	IForest	7.99 \pm 4.2	1167	0.46	0.744 \pm 0.22	0.33
	EGMM	5.57\pm3.8	1195	0.64	0.828\pm0.20	0.22
	DTE-NP	5.94 \pm 3.4	1233	0.61	0.816 \pm 0.19	0.25
Deep	GOAD	11.27 \pm 3.4	581	0.21	0.590 \pm 0.24	0.40
	ICL	7.26\pm3.5	951	0.43	0.770\pm0.20	0.29
	DTE-C	7.26\pm3.5	939	0.43	0.770\pm0.19	0.29
	NPT-AD	10.31 \pm 4.2	356	0.28	0.627 \pm 0.26	0.38
FM	TabPFN-OD	6.22 \pm 4.0	877	0.59	0.815 \pm 0.20	0.23
	FoMo-OD	7.18 \pm 4.5	997	0.52	0.783 \pm 0.21	0.26
	OutFormer	5.88\pm3.9	1039	0.61	0.821\pm0.19	0.21

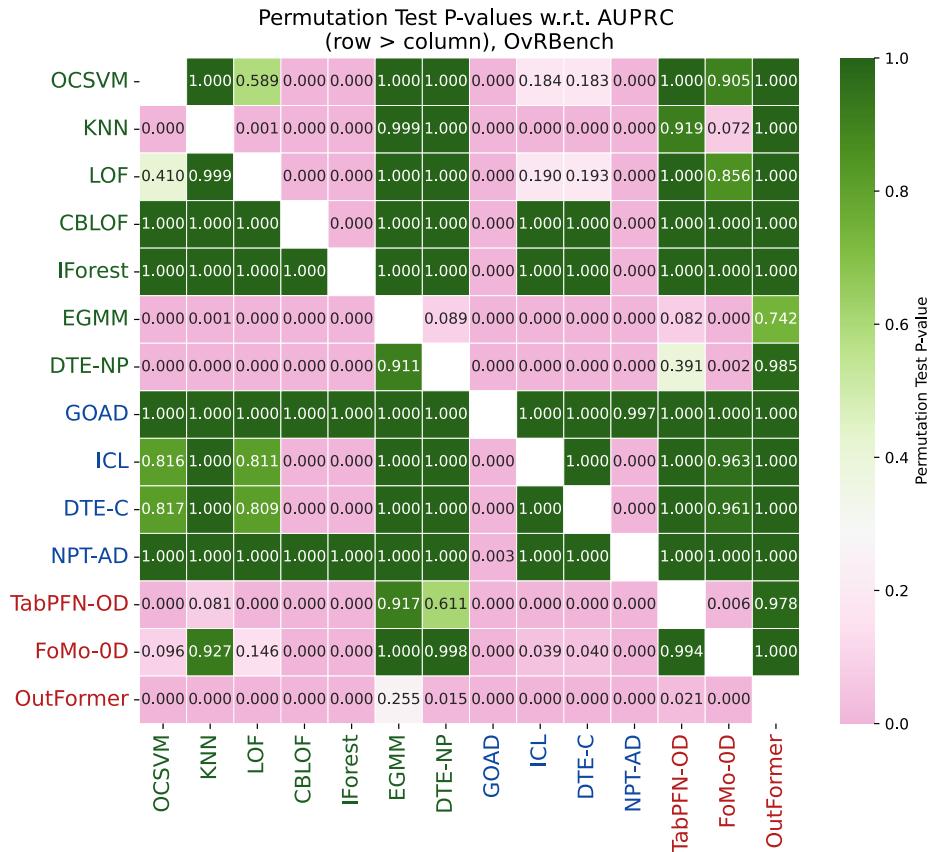


Figure 16: Paired permutation test results w.r.t. AUPRC across 756 public OvRBench datasets. All foundation models achieve strong performance (last three rows), with OUTFORMER outperforming all baselines significantly ($p \leq 0.05$), except EGMM ($p = 0.255$). Deep models do not achieve competitive results, mainly due to hyperparameter sensitivity.

Table 13: Overall AUPRC performance comparison across models on the public partition of SynBench (800 datasets). Colors depict OD method categories, where green, blue, and red respectively denote shallow (classical), deep, and foundation models. Best results of each category are shown in bold, while global best is underlined. OUTFORMER and TABPFN-OD achieve the strongest overall results, significantly outperforming the rest of the baselines.

	Model	Avg. Rank (\downarrow)	ELO (\uparrow)	Winrate (\uparrow)	rAUC (\uparrow)	C_{Δ} (\downarrow)
Shallow	OCSVM	10.77 \pm 1.8	370	0.25	0.687 \pm 0.16	0.88
	KNN	6.77 \pm 2.2	1036	0.54	0.800 \pm 0.18	0.74
	LOF	4.92 \pm 1.9	1266	0.68	0.855 \pm 0.15	0.69
	CBLOF	9.37 \pm 2.8	893	0.34	0.638 \pm 0.30	0.80
	IForest	12.02 \pm 1.6	633	0.15	0.553 \pm 0.30	0.89
	EGMM	3.40\pm2.1	1538	0.80	0.931\pm0.11	0.53
	DTE-NP	6.47 \pm 1.9	1026	0.56	0.814 \pm 0.17	0.75
Deep	GOAD	11.23 \pm 2.2	673	0.21	0.591 \pm 0.29	0.87
	ICL	8.31 \pm 2.8	1181	0.44	0.744 \pm 0.21	0.81
	DTE-C	5.58\pm2.8	1091	0.64	0.904\pm0.10	0.71
	NPT-AD	13.43 \pm 1.3	56	0.04	0.426 \pm 0.25	0.92
FM	TabPFN-OD	3.51 \pm 3.5	<u>1601</u>	0.79	0.920 \pm 0.17	<u>0.29</u>
	FoMo-OD	5.01 \pm 2.7	1280	0.68	0.885 \pm 0.14	0.63
	OutFormer	<u>3.34\pm3.1</u>	1356	<u>0.82</u>	<u>0.984\pm0.04</u>	0.41

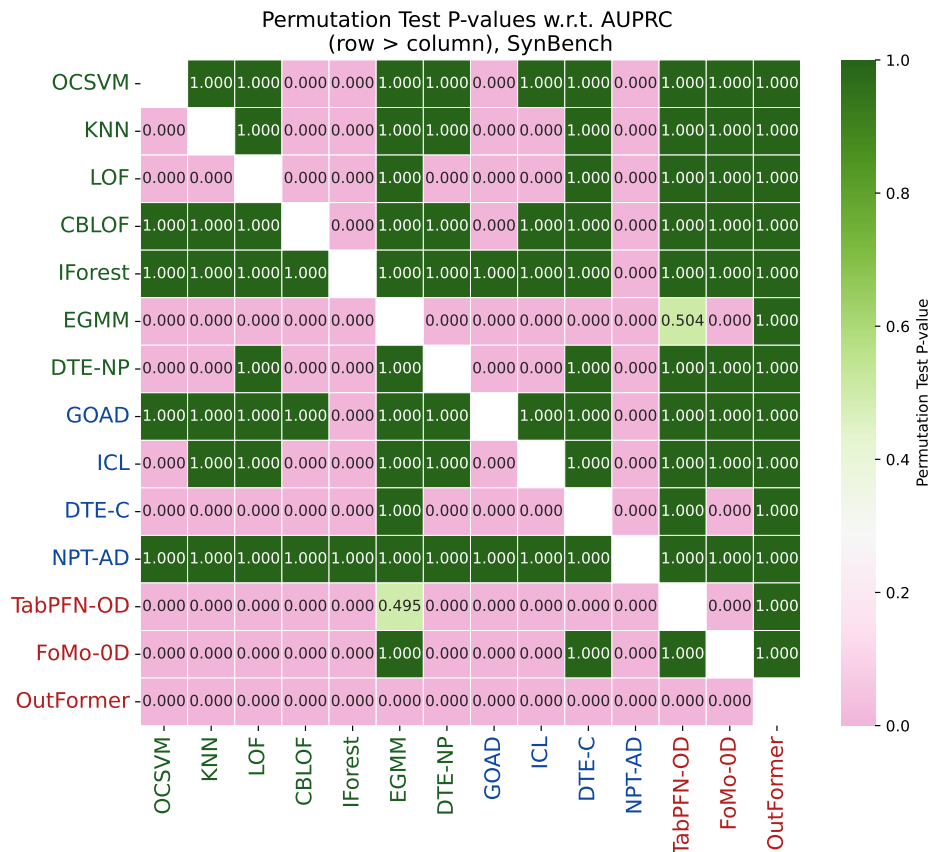


Figure 17: Paired permutation test results w.r.t. AUPRC across 800 public SynBench datasets. All foundation models achieve competitive performance (last three rows), with OUTFORMER outperforming all baselines significantly ($p \leq 0.05$).

Table 14: Overall AUROC performance comparison across models on the public partition of OddBench (690 datasets). Colors depict OD method categories, where green, blue, and red respectively denote shallow (classical), deep, and foundation models. Best results of each category are shown in bold, while global best is underlined. OUTFORMER and DTE-NP achieve the strongest overall performance, with foundation models generally offering the leading edge.

	Model	Avg. Rank (\downarrow)	ELO (\uparrow)	Winrate (\uparrow)	rAUC (\uparrow)	C_{Δ} (\downarrow)
Shallow	OCSVM	7.44 \pm 3.0	1007	0.49	0.871 \pm 0.11	0.52
	KNN	6.10 \pm 3.4	990	0.58	0.879 \pm 0.15	0.43
	LOF	7.14 \pm 4.0	954	0.50	0.848 \pm 0.16	0.50
	CBLOF	7.73 \pm 3.5	958	0.46	0.853 \pm 0.14	0.50
	IForest	7.43 \pm 3.9	865	0.50	0.865 \pm 0.13	0.50
	EGMM	5.73 \pm 4.2	1018	0.61	0.868 \pm 0.19	0.37
	DTE-NP	5.44\pm3.4	1140	0.64	0.891\pm0.15	0.41
Deep	GOAD	11.31 \pm 3.7	731	0.19	0.658 \pm 0.23	0.64
	ICL	8.68 \pm 3.5	944	0.40	0.828 \pm 0.15	0.55
	DTE-C	7.11\pm3.7	1126	0.51	0.860\pm0.16	0.48
	NPT-AD	10.33 \pm 4.0	642	0.28	0.736 \pm 0.20	0.59
FM	TabPFN-OD	6.07 \pm 4.0	1200	0.58	0.886 \pm 0.14	0.39
	FoMo-OD	7.02 \pm 4.5	1165	0.51	0.857 \pm 0.16	0.43
	OutFormer	5.62\pm3.9	1262	0.61	0.889\pm0.14	0.37

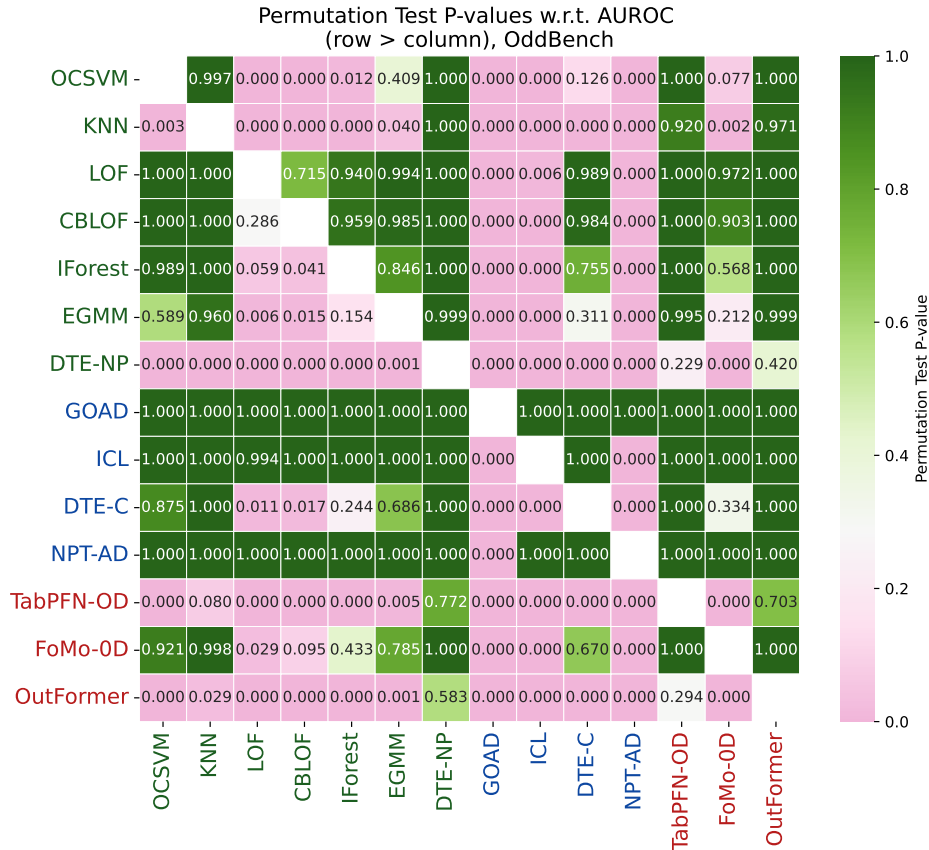


Figure 18: Paired permutation test results w.r.t. AUROC across 690 public OddBench datasets. Among shallow methods, DTE-NP emerges as the strongest performer, followed by EGMM and KNN. Deep models generally underperform, mainly due to their hyperparameter sensitivity. Foundation models OUTFORMER and TABPFN-OD achieve strong performance, both outperforming all other baselines significantly ($p \leq 0.05$), except DTE-NP ($p = 0.583$ and $p = 0.772$, respectively).

Table 15: Overall AUROC performance comparison across models on the public partition of OvRBench (756 datasets). Colors depict OD method categories, where green, blue, and red respectively denote shallow (classical), deep, and foundation models. Best results of each category are shown in bold, while global best is underlined. The shallow methods KNN, EGMM, and DTE-NP, as well as the foundation models OUTFORMER and TABPFN-OD achieve the strongest overall results, significantly outperforming the rest of the baselines while being comparable among themselves.

	Model	Avg. Rank (\downarrow)	ELO (\uparrow)	Winrate (\uparrow)	rAUC (\uparrow)	C_{Δ} (\downarrow)
Shallow	OCSVM	7.71 \pm 3.2	1125	0.47	0.890 \pm 0.09	0.40
	KNN	6.01 \pm 3.5	1274	0.60	0.907\pm0.12	0.30
	LOF	7.04 \pm 3.8	1033	0.52	0.874 \pm 0.15	0.37
	CBLOF	7.60 \pm 3.5	1230	0.48	0.886 \pm 0.12	0.38
	IForest	7.30 \pm 4.0	1223	0.51	0.895 \pm 0.11	0.37
	EGMM	5.66\pm4.0	1217	0.63	0.906 \pm 0.14	0.28
	DTE-NP	5.85 \pm 3.5	1211	0.62	0.906 \pm 0.12	0.31
Deep	GOAD	11.48 \pm 3.5	403	0.19	0.704 \pm 0.20	0.55
	ICL	6.76\pm3.4	1021	0.47	0.885\pm0.12	0.36
	DTE-C	6.76\pm3.4	1009	0.47	0.885\pm0.12	0.36
	NPT-AD	10.57 \pm 3.9	443	0.26	0.777 \pm 0.16	0.49
FM	TabPFN-OD	6.39 \pm 4.0	880	0.57	0.903\pm0.12	0.30
	FoMo-OD	7.74 \pm 4.4	907	0.47	0.867 \pm 0.14	0.37
	OutFormer	6.15\pm4.0	1024	0.59	0.903\pm0.11	0.29

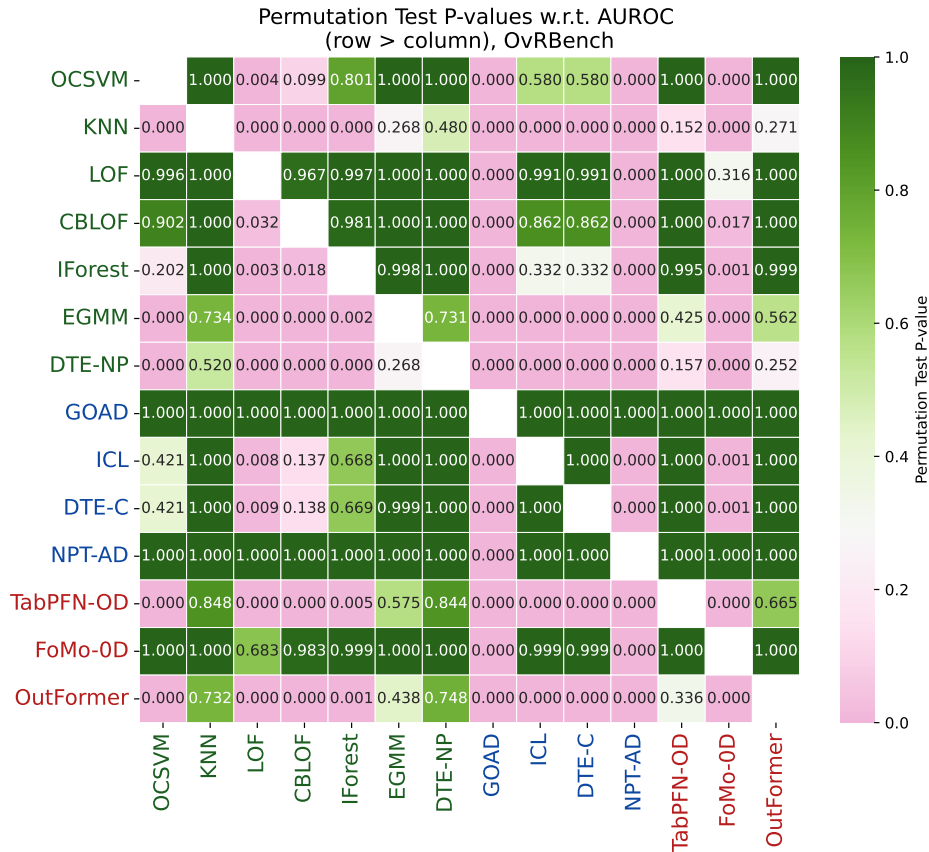


Figure 19: Paired permutation test results w.r.t. AUROC across 756 public OvRBench datasets. Among shallow models, EGMM, DTE-NP and KNN achieve strong and comparable performance, which are also statistically similar to two foundation models, OUTFORMER and TABPFN-OD.

Table 16: Overall AUROC performance comparison across models on the public partition of SynBench (800 datasets). Colors depict OD method categories, where **green**, **blue**, and **red** respectively denote shallow (classical), deep, and foundation models. Best results of each category are shown in bold, while global best is underlined. **OUTFORMER**, **TABPFN-OD** and **EGMM** achieve the strongest overall results, significantly outperforming the rest of the baselines.

	Model	Avg. Rank (↓)	ELO (↑)	Winrate (↑)	rAUC (↑)	C _Δ (↓)
Shallow	OCSVM	11.30 _{±1.6}	397	0.21	0.827 _{±0.07}	0.91
	KNN	6.52 _{±2.1}	1039	0.55	0.929 _{±0.07}	0.73
	LOF	5.18 _{±2.1}	1151	0.65	0.941 _{±0.06}	0.68
	CBLOF	9.68 _{±3.0}	874	0.31	0.839 _{±0.14}	0.80
	IForest	11.42 _{±1.7}	698	0.20	0.817 _{±0.14}	0.89
	EGMM	3.09_{±2.0}	1515	0.81	0.978_{±0.04}	0.47
	DTE-NP	5.84 _{±1.9}	1066	0.60	0.932 _{±0.07}	0.72
Deep	GOAD	11.44 _{±2.2}	556	0.19	0.800 _{±0.13}	0.89
	ICL	8.46 _{±2.7}	1178	0.42	0.888 _{±0.10}	0.82
	DTE-C	5.01_{±2.5}	1415	0.67	0.966_{±0.04}	0.67
	NPT-AD	13.55 _{±1.3}	138	0.03	0.664 _{±0.16}	0.94
FM	TabPFN-OD	3.36 _{±3.2}	<u>1522</u>	0.79	0.969 _{±0.07}	0.30
	FoMo-OD	5.34 _{±2.8}	1104	0.65	0.950 _{±0.06}	0.63
	OutFormer	3.30_{±2.8}	1347	0.81	0.993_{±0.01}	0.42

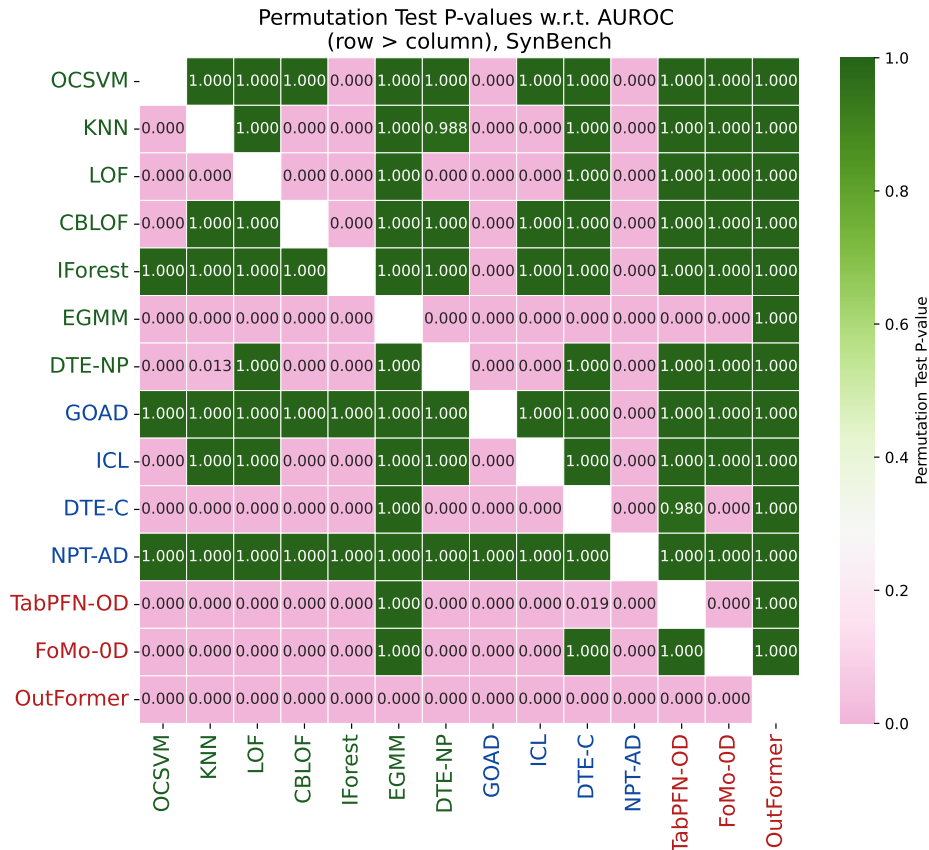


Figure 20: Paired permutation test results w.r.t. AUROC across 800 public SynBench datasets. EGMM is the strongest performer among shallow and deep methods. Foundation models achieve competitive performance (last three rows), with **OUTFORMER** outperforming all baselines significantly ($p \leq 0.05$).

Table 17: AUROC performance comparison across models on overall 2,446 datasets across three benchmarks.. Colors depict OD method categories, where **green**, **blue**, and **red** respectively denote shallow (classical), deep, and foundation models. Best results of each category are shown in bold, while overall best is underlined.

	Model	Avg. Rank (\downarrow)	ELO (\uparrow)	Winrate (\uparrow)	rAUC (\uparrow)	C_{Δ} (\downarrow)
Shallow	OCSVM	8.91 \pm 3.2	397	0.38	0.862 \pm 0.09	0.62
	KNN	6.22 \pm 3.1	1037	0.57	0.906 \pm 0.12	0.49
	LOF	6.41 \pm 3.5	1153	0.56	0.890 \pm 0.13	0.52
	CBLOF	8.38 \pm 3.5	874	0.41	0.859 \pm 0.13	0.57
	IForest	8.81 \pm 3.8	699	0.40	0.858 \pm 0.13	0.59
	EGMM	4.76\pm3.7	1521	0.69	0.920\pm0.14	0.38
	DTE-NP	5.72 \pm 3.0	1066	0.62	0.911 \pm 0.12	0.49
Deep	GOAD	11.41 \pm 3.2	557	0.19	0.724 \pm 0.20	0.70
	ICL	7.95 \pm 3.3	1176	0.43	0.869 \pm 0.13	0.58
	DTE-C	6.24\pm3.4	1411	0.55	0.906\pm0.12	0.51
	NPT-AD	11.56 \pm 3.6	138	0.18	0.724 \pm 0.18	0.68
FM	TabPFN-OD	5.21 \pm 4.0	<u>1522</u>	0.65	0.921 \pm 0.12	0.33
	FoMo-OD	6.67 \pm 4.1	1108	0.55	0.894 \pm 0.13	0.48
	OutFormer	4.97\pm3.8	1342	0.68	0.931\pm0.11	0.36

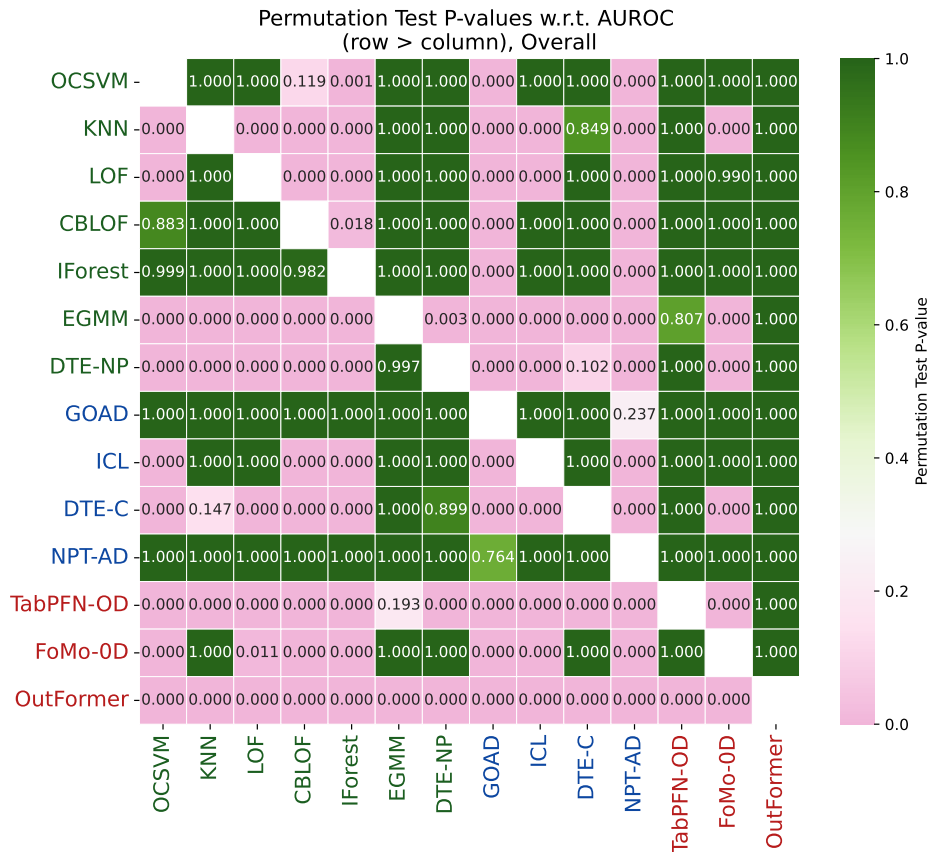
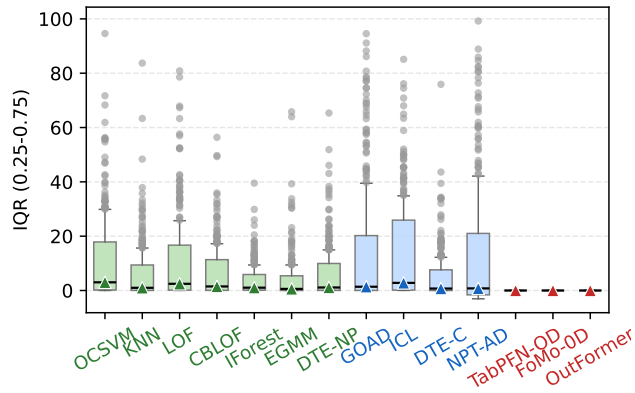
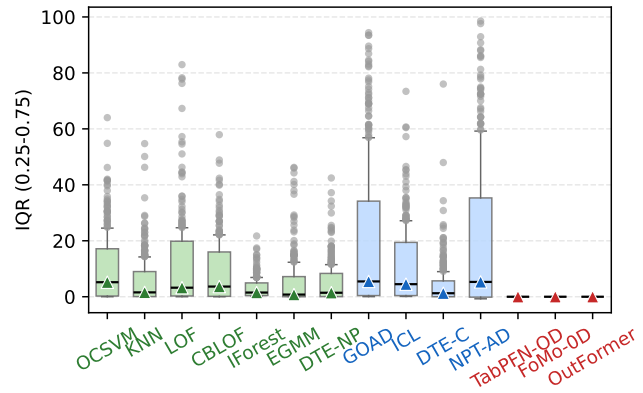


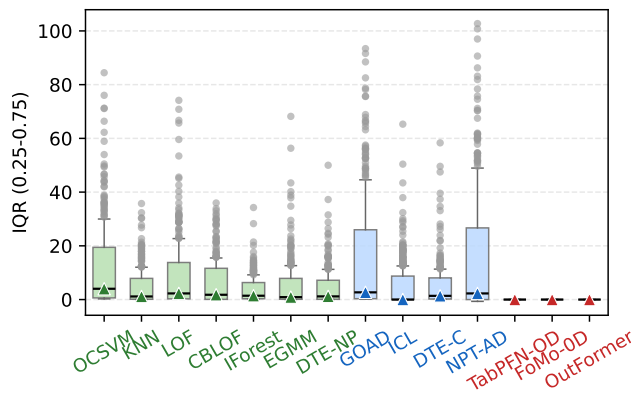
Figure 21: Paired permutation test results w.r.t. AUROC across overall 2,446 datasets. Foundation models (last three rows) demonstrate competitive performance, as well as classical methods EGMM and DTE-NP while the latter being much slower. OUTFORMER significantly outperforms all baselines ($p \leq 0.05$).



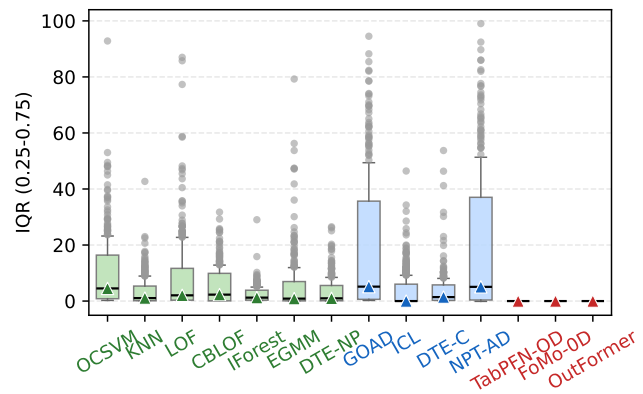
(a) AUPRC on OddBench



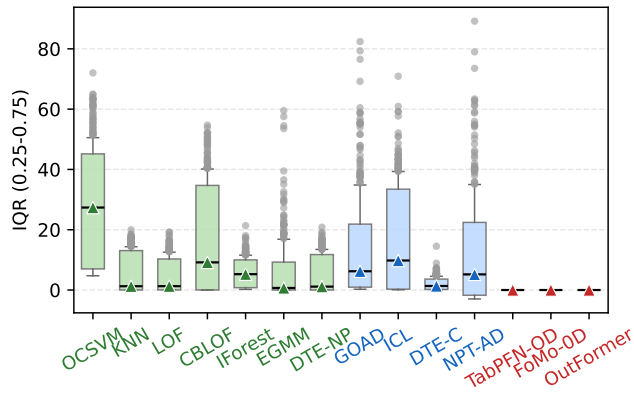
(b) AUROC on OddBench



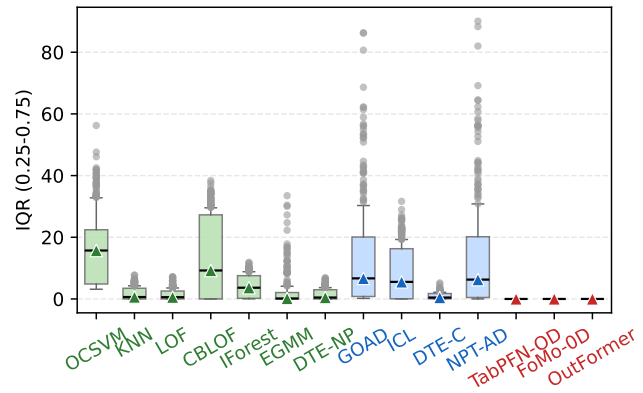
(c) AUPRC on OvRBench



(d) AUROC on OvRBench



(e) AUPRC on SynBench



(f) AUROC on SynBench

Figure 22: Hyperparameter sensitivity as measured by inter-quartile 25%-75% performance; the higher, the more HP-sensitive. Subfigures (a)–(f) report AUPRC and AUROC performance variation under different hyperparameter configurations across all datasets (boxplot) per baseline, on OddBench, OvRBench, and SynBench.

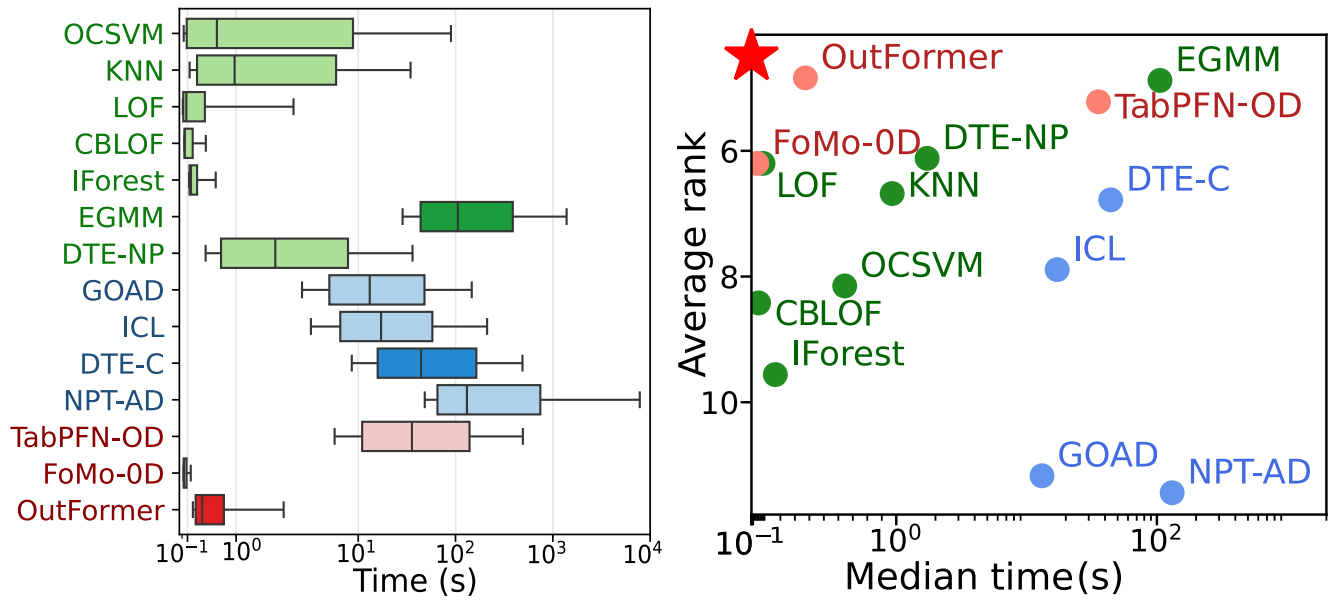


Figure 23: (left) Running time comparison of OD methods across all datasets. Feed-forward-only foundation models (FMs) incur as low latency as certain shallow models such as iForest, while achieving significantly better performance. Deep models take considerably longer, while competitive shallow models EGMM, DTE-NP and kNN are also slow relative to FMs. (right) Median total time (fitting+inference) vs. Avg rank w.r.t. AUPRC across all 2,446 datasets combined. Foundation models FoMo-0D and OutFormer occupy the Pareto front, offering the best overall performance-time trade-off. EGMM and DTE-NP achieve competitive performance while taking considerable running time.